Earth Syst. Sci. Data Discuss., https://doi.org/10.5194/essd-2018-50
Manuscript under review for journal Earth Syst. Sci. Data
Discussion started: 24 April 2018

Open Access Earth System Science Data Discussions

SURATLANT: a 1993-2017 surface sampling in the central part of the North Atlantic subpolar gyre

GillesReverdin[1], NicolasMetzl[1], SolveigOlafsdottir[2], VirginieRacapé[3], TaroTakahashi[4], MarionBenetti[5], HedinnValdimarsson[2], AliceBenoit-Cattin[2], MagnusDanielsen[2], JonathanFin[1], AichaNaamar[1], DenisPierrot[6], KevinSullivan[6], Francis Bringas[6], Gustavo Goni[6]

[1]Sorbonne Université/CNRS/IRD/MNHN, Laboratoire d'océanographie et du climat : expérimentations et approches numériques (LOCEAN), Paris, France

[2]Marine and Freshwater Research Institute, Reykjavik, Iceland

[3] Laboratoire d'Océanographie Physique et Spatiale (LOPS), CNRS/Ifremer/IRD/UBO-IUEM, Brest, France

[4]Lamont-DohertyEarth Observatory (LDEO), Columbia University, Palisades, NY, USA

[5]Institute of Earth Sciences, University of Iceland, Reykjavik, Iceland

[6]National Oceanic and Atmospheric Administration/Atlantic Oceanographic and Meteorological Laboratory, Miami, Florida, USA

Earth Syst. Sci. Data Discuss., https://doi.org/10.5194/essd-2018-50
Manuscript under review for journal Earth Syst. Sci. Data
Discussion started: 24 April 2018

Open Access Earth System Science Data Discussions

Abstract

This paper presents the SURATLANT dataset (SURveillance ATLANTique), consisting of individual data of temperature, salinity, parameters of the carbonate system, nutrients and water stable isotopes ($\delta^{18}O$ and δD) collected mostly from ships of opportunity since 1993along transects between Iceland and Newfoundland (doi:10.17882/54517). We discuss how the data are validated, qualified, their accuracy and the overall characteristics of the data set. The data are used to reconstruct seasonal cycles and interannual anomalies, in particular of Sea Surface Salinity (SSS), inorganic nutrients, dissolved inorganic carbon (DIC) and its isotopic composition $\delta^{13}C_{DIC}$, total alkalinity (A_t), and water isotope concentrations. Derived parameters, such as fCO_2 and pH are also estimated. The relation between salinity and A_t is estimated in these data to investigate the possibility to replace missing A_t when estimating other parameters of the carbonate system. We compare the seasonal cycle derived from these data with other climatologies. We find a period of small seasonal change between January and late April, except on the Newfoundland shelf/continental slope, when changes related with spring-stratification and blooms occur earlier. The data were collected in a period of multi-decennial variability associated with the Atlantic meridional oscillation with warming between 1994and 2004-2007, and the recent cooling having peaked in 2014-2016. We also observe strong salinification in 2004-2009 and fresher waters in 1994-1995 as well as since 2010 south of 54°N and in 2016-2017north of 54°N. Indication of multi-decadal variability is also suggested by other variables, such as phosphate or DIC, but cannot be well resolved seasonally with the discrete sampling and in the presence of interannual variability. As a whole, over the 24 years ocean fCO_2 trend ($+1.9 \mu atm yr^{-1}$) is close to the atmospheric trend and associated with an increase in DIC ($+0.70\ \mu mol kg^{-1}\ yr^{-1}$). The data also revealed a "canonical" pH decrease of $-0.002 yr^{-1}$. There is also a decrease in $\delta^{13}C_{DIC}$between 2005 and 2017 (in winter, $-0.015‰ yr^{-1}$, but larger in summer, $-0.042‰ yr^{-1}$), suggesting significant anthropogenic carbon signal at play together with other processes (mixing, biological activity).

Data availability

The data set is freely available and is accessible at http://www.seanoe.org/data/00434/54517/ (doi:10.17882/54517)

Earth Syst. Sci. Data Discuss., https://doi.org/10.5194/essd-2018-50
Manuscript under review for journal Earth Syst. Sci. Data
Discussion started: 24 April 2018

Open Access Earth System Science Data Discussions

1 Introduction

The North Atlantic subpolar gyre is a major site for formation of intermediate and deep waters, and thus plays a key role in the ocean meridional overturning circulation. The upper ocean circulation brings to its southern and eastern parts relatively warm and salty water of subtropical origin. This water is then cooled by large heat loss to the atmosphere and freshened by local excess precipitation as well as by inputs of fresher water from the Arctic or from continental and ice cap origin (Boyer et al., 2007). Part of this upper water then flows into the Nordic Seas, whereas the other part recirculates cyclonically in the gyre, steered by topography, such as around the Reykjanes Ridge (Fig. 1) and progressively transformed by winter mixing into intermediate waters in the Labrador and Irminger Seas or further entrained in the dense outflows of the Nordic Seas to form Atlantic deep waters (Mercier et al., 2015; Daniault et al., 2016; Rossby et al., 2017).

This region is the only large part of the world ocean which has experienced a surface cooling trend over the last century (Rahmstorf et al., 2015), which some have linked to changes in the meridional overturning circulation and to an observed overall surface freshening (Friedman et al., 2017). It also experiences very large decadal to multi-decadal variability (Yashayaev and Loder, 2016; Reverdin, 2010; Frajka-Williams et al., 2017; Robson et al., 2016) associated with Atlantic Multi-decadal variability. This might result from atmospheric variability, as well as by changes in the strength of the Meridional Overturning Circulation (Häkkinen and Rhines, 2004; Häkkinen et al., 2011; Hátún et al., 2005; Reverdin, 2010; Chafik et al., 2016). The most recent trend has been a large cooling and freshening since 2005, which reversed a previous warming and freshening since the mid-1990s (Robson et al., 2016). It was associated in 2014-2015 with particularly strong positive NAO atmospheric conditions inducing large vertical mixing and deep convection in the Labrador Sea and the Irminger Sea (Yashayaev and Loder, 2016; Piron et al., 2017; de Jong and de Steur, 2016; Fröb et al., 2017).

The North Atlantic contributes substantially to the global oceanic uptake of CO_2, mainly due to extensive biological activity during summer and considerable heat loss during winter, as well as by the export of surface waters to the deep ocean by the ocean circulation and vertical mixing. As a result, large anthropogenic carbon inventory is evaluated in this region (e.g. Khatiwala et al 2013; Zunino et al., 2014). Takahashi et al. (2009) estimate that the annual mean air-sea CO_2 flux in the North Atlantic, north of 50° N (representing only 5% of the ocean surface), is 0.27 Pg yr^{-1}, i.e. almost 20% of the

Earth Syst. Sci. Data Discuss., https://doi.org/10.5194/essd-2018-50
Manuscript under review for journal Earth Syst. Sci. Data
Discussion started: 24 April 2018

global flux. Although the mean annual carbon flux is a robust result for the North Atlantic (Takahashi et al. 2002, 2009; Watson et al., 2009; Schuster et al, 2013) there is still disagreement in the magnitude of seasonal, interannual to decadal variability depending on the method used to evaluate air-sea CO_2 fluxes (Schuster et al., 2013). Compared to other basins, the air-sea CO_2 fluxes interannual variability in the North Atlantic appears relatively small (Rödenbeck et al., 2015; Landschützer et al., 2016), although during some periods, significant variability has been recognized at regional scale in the NASG (North Atlantic Subarctic Gyre) related to either warming or deep convection (Corbière et al., 2007; Metzl et al., 2010; Rödenbeck et al., 2014). The variations of winds would impact on air-sea CO_2 fluxes (Wanninkhof and Trinanes, 2007), but at long-term they are mainly controlled by the rate of change of ocean fCO_2 versus atmospheric concentrations. Based on a synthesis of pCO_2 observations for years 1972-2006, Takahashi et al (2009) evaluate a mean rate of 1.8 $\mu atm yr^{-1}$ (+/- 0.4) in the North Atlantic, i.e. close to atmospheric increase, a result revisited and confirmed by McKinley et al. (2011) for the period 1981-2009. An analysis of recent data (2005-2014) across the NASG near 59-60°N also suggests surface fCO_2 trends that are near the atmospheric increase (Fröb et al., 2018a). Interestingly, this study also illustrates a spatial variety of the mechanisms for these trends. For example,Fröb et al. (2018a) found onlyin the Iceland Basin a large contribution of alkalinity changes related to a salinity decrease.

The uptake of CO_2 through air-sea gas exchange affects the seawater CO_2 chemistry and leads to ocean acidification (Gattuso and Hansson, 2011). Over the past two decades, the pH in North Atlantic surface waters has declined at a similar rate as global ocean pH (-0.0018 yr^{-1}) (Lauvset et al., 2015; García-Ibáñez et al., 2016). However, in a similar way as for fCO_2, the pH interannual variability could be significant at regional scale. As an extreme case, based on the winter 2001-2008 SURATLANTdata, Metzl et al. (2010) reported a pH rate of -0.0069yr^{-1} associated witha particularly fast rise of oceanic fCO_2 (up to 7.2 $\mu atm yr^{-1}$).

Finally, the large uptake of anthropogenic CO_2 in the ocean leads to a strong change in the isotopic composition of dissolved inorganic carbon (DIC) reducing thus its $^{13}C/^{12}C$ ratio (noted $\delta^{13}C_{DIC}$ hereafter). The $\delta^{13}C_{DIC}$ decrease in response to the human-induced perturbation is less than -0.007‰yr^{-1} in polar surface regions (McNeil et al., 2001; Olsen et al., 2006) and reaches-0.025‰yr^{-1} in subtropical regions (Gruber et al., 1999), observations which has been used to validate oceanic models for these regions (Tagliabue and Bopp, 2008; Sonnerup and Quay, 2012). This decrease is generally masked by the seasonal cycle due to physical and biological mechanisms, which is as large as

Earth Syst. Sci. Data Discuss., https://doi.org/10.5194/essd-2018-50
Manuscript under review for journal Earth Syst. Sci. Data
Discussion started: 24 April 2018

1‰ in the NASG (Gruber et al., 1999; Racapé et al., 2014). Although $\delta^{13}C_{DIC}$ provides additional information allowing us to further understand mechanisms of ocean region CO_2 uptake in key region as NASG, its interannual to decadal variability is still poorly documented.

In order to unravel the surface NASG variability, it is necessary to revisit the region studied by (Corbière et al., 2007; Metzl et al., 2010; Racapé et al., 2014) with a more comprehensive data set. The 24years of physical and geochemical data presented here cover the recent multi-decadal sea-saw of warming/cooling and will provide an alternate view on the decadal variability in fCO_2 and pH in the central part of the NASG. The data set encompasses temperature (T), salinity (S), water stable isotopes, dissolved inorganic carbon (DIC), total alkalinity (A_t), nutrients, $\delta^{13}C_{DIC}$. fCO_2 and pH are computed from these data.

The data have been binned in time and in latitude bands for later use. The data and the binning method are first presented (section 2). To illustrate the properties of the data set, we will then present the average seasonal cycle (section 3), as well as first order estimates of trends over the whole period (section 4).

2 Data and Methods

2.1 Data

Data were collected since 1993 along different container vessels operated or leased by EIMSKIP, mostly between Reykjavik (Iceland) and Argentia (southern Newfoundland). The ships most commonly crossed the North Atlantic in nearly 5 days first close to the Reykjanes ridge or to its west reaching the Newfoundland slope southwest of 49°N/49°W (AX02 transect on Fig.1). However weather (late autumn to early spring) and ice conditions (January-April) often influence the ship's route, so that it can also cross the central Irminger Sea or intersect meanders of the North Atlantic Current (NAC), further to the southwest. The sampling used here is largely based on the collection of surface samples collected by ship riders sent every three months. In addition, the ships have been equipped a large part of the time with a SBE21 thermosalinograph (TSG)between April 1994 and May 2007 and a SBE45 micro TSG with an external temperature sensor SBE38 between February 2011 and March 2016,as well as by a fCO_2equilibration system by NOAA/AOML (R. Wanninkhof, D. Pierrot) in 2003-2007 and 2013-2016 (data are in SOCAT database (Bakker et al., 2016) and at http://www.aoml.noaa.gov/ocd/ocdweb/occ.html), both installed on a water circuit pumping water at depths of 4-6m. Expendable bathythermograph (XBT) probes have also regularly been deployed

Earth Syst. Sci. Data Discuss., https://doi.org/10.5194/essd-2018-50
Manuscript under review for journal Earth Syst. Sci. Data
Discussion started: 24 April 2018

regularly along the AX02 transect (Fig. 1) (profiles from approximately 12000 temperature probes collected between November 2008 and April 2016 at approximately 25 km resolution during these transects are available on NOAA/AOML site http://www.aoml.noaa.gov/phod/hdenxbt/index.php). The validation and correction of the TSG salinity data has been done by one of the authors, mostly based on comparison with the water samples collected from a water intake at the TSG and also using nearby upper level of Argo float data (see also, Alory et al., 2015). Except in April 1994-April 1996T was measured at an intake. In July 1993 to January 1994 and in 2017, T was measured directly in the sea from a bucket. At other times, it is T measured by the TSG that was adjusted to estimate ocean T, by correcting warming in pipes based on comparison with 5-m temperatures from XBTs deployed along the transects. The validated T/S data from the TSG are archived in the SSS repository at LEGOS (www.legos.obs-mip.fr/SSS). In addition, we include data collected during one transect on the R.V. Thalassa during the RREX2017 cruise in July/August 2017 in the same region, for which there were intake temperatures associated with the TSG data.

The surface samples were usually collected from an intake corresponding to water pumped between 4 and 7-m depending on the vessel depth (except in 06/1993 and 01/1994, when water was collected with a bucket and its temperature measured by a calibrated thermometer). T is usually reported with the samples. Most commonly, it originates from the temperature measured by the TSG (and adjusted as reported above) or from bucket T measurements. During some cruises, T values were complemented using T from XBTs deployed as close to the time and location of those records as possible. In rarer occasions, SSM/I satellite-derived microwave SSTs collocated at the ship time and position were used, and for two transects in 07/2016 and 10/2016, upper-level T from nearby Argo profiles were also used as a proxy. Initially in 1993, the water collection included samples for S, DIC, $\delta^{18}O$ of sea water and inorganic phosphate. These were analysed at LDEO, but due to GR moving to France, the sample analysis was progressively discontinued (inorganic phosphate in late 1994, $\delta^{18}O$ of sea water in late 1995, and DIC in February 1997),and then moved to other centres. Salinity sampling was never discontinued and S has been analysed since 2000 in Reykjavik (MFRI). DIC and A_t have been analysed at LODYC/LOCEAN in Paris since June 2001, and inorganic nutrients (nitrate+nitrite, phosphate, silicic acid; later reported as NO_3, PO_4, Si) since December 2001 in Reykjavik (MFRI). Water stable isotopes of sea water ($\delta^{18}O$ and δD) have been analysed since late 2011mostly at LOCEAN in Paris (some of these data are presented in Benetti et al. (2016), but with emphasis on the subset on Newfoundland shelf and slope). Finally, $\delta^{13}C_{DIC}$ has been analysed in 2005/2006 at the Univ. of

Earth Syst. Sci. Data Discuss., https://doi.org/10.5194/essd-2018-50
Manuscript under review for journal Earth Syst. Sci. Data
Discussion started: 24 April 2018

Washington and since 2010 at LOCEAN (Racapé et al., 2014).Units are standard ones. Conversion was done for nutrients from measurements in μmol l^{-1} into μmol kg^{-1}assuming measurements conducted at 25°C. The water stable isotopes ($\delta^{18}O$ and δD) are reported as concentration in VSMOW scale (Benetti et al., 2017), whereas salinity is expressed as a practical salinity (on plots, psu is sometimes mentioned to indicate that this is reported in the practical salinity scale).

Details on data collection, validation and accuracy are provided in App. A. Part of the DIC/A_t and nutrient data (1993-2013) have been made available through the PANGEAE database (Reverdin et al.,2007, 2015), whereas most of the water isotope data have been contributed to the GISS database.

The seawater CO_2 chemistry can be fully described with the measured DIC and A_t, using the dissociation constants of Lueker et al. (2000) as implemented in CO2SYS (Lewis and Wallace, 1998;Pierrot et al., 2006). Estimating fCO_2 or pH from these equations also requires T and S data (see above), as well as nutrients. When nutrient data are missing, we use the climatology derived from all the data at the calendar date of the sampling. The error in doing it has little impact on the computation. When no A_t was measured with DIC such as before 2001, we use parameterized A_t based on salinity. The strong correlation between sea surface alkalinity and salinity in the open ocean can be described with an empirical linear relationship (Millero et al., 1998; Friis et al., 2003). In our previous analysis we used a relation based on seasonal SURATLANT data but only for years 2001-2002 (Corbière et al., 2007; Metzl et al., 2010)

At = 45.808 × S + 713.5, (r^2=0.92, RMSD = ±10.3 μmolkg^{-1}).

Here, an updated formula is derived for S > 34 based on all the reported SURATLANT data in 2001-2016.

$A_t = 46.2543 * S + 687.74; (SSS > 34.0)$($r^2$=0.84, RMSD = ±8.4 μmol$kg^{-1}$)

This relation is close to the one derived by Nondal et al. (2009) for the North Atlantic:

$$A_t = 49.35 * S + 582; (SSS > 34.5)$$

Our formula which has a larger 0-crossing explains a large part of the variance in A_t, at least for S larger than 34 psu (Fig. 2). For the lower salinities found on the Newfoundland shelf, different sources of freshwater (from the Arctic or resulting from continental or sea ice melt inputs) contribute to deviations from the relation. The impact on fCO_2 or pH of using this relationship instead of others or

measured A_t is discussed in App. B.

Trends in sea water fCO_2 will be compared to trends in atmospheric fugacity. Atmospheric CO_2 mean mole fraction data were provided by the Cooperative Global Atmospheric Data Integration Project (2016). Here, the xCO_2 data collected at Mace Head, Ireland (53.3° N) were used, after some editing (mostly when wind from land). The xCO_2 data were converted to fugacities at 100% humidity following Weiss and Price [1980].The xCO_2 trend at Mace Head is1.9 ppm/year in 1993-2016, increasing to 2.1 ppm/year in 2006-2016 which is coherent with global average trends (e.g. Le Quéré et al. 2018). Local values of atmospheric fCO_2 can present significant spatial differences at subpolar latitudes depending on wind regimes, but that is unlikely to have had a strong influence on the long-term trends that are indicated here for reference purpose.

2.2 Methods

2.2.1 Binning the time series

T and S anomaly time series are presented as Hövmüller diagrams in App. C. The sample data reproduce part of this long term variability, albeit with an insufficient sampling to properly separate the interannual variability from longer term changes. The discrete sampling also results in uncertainties in estimating a seasonal cycle, in particular for parameters such as $\delta^{13}C_{DIC}$ or $\delta^{18}O$ which have been sampled for less time.

To reduce uncertainties in estimating an average seasonal cycle, we first remove from individual data an expected dependency in S estimated by linear regression for A_t, DIC, $\delta^{18}O$ and δD (as done in Friis et al., 2013). For A_t, this is the A_t-S regression mentioned above, and for water stable isotopes, as done in (Benetti et al., 2016). For nutrients, we normalize by S/35. We then also remove an average trend for DIC over 1993-2017 and for $\delta^{13}C_{DIC}$ over 2005-2017, as estimated from the whole data set (see section 4). Then, we bin the data in five 4° boxes from 46-50°N to 62-64°N roughly (see boxes on Fig. 3). The southern box covers the shelf and slope area and incorporates only samples for which S<34.1. The next box from 50-54°N incorporates only samples with S between 34 and 35 to avoid including shelf water or from the North Atlantic Current (NAC). 54°N is near the shift in S variability observed in the data (cf App. C), and thus separates box 2 from 3. We also remove data collected too far west in the western Irminger Sea or central Labrador Sea as well as too far east in the western Iceland Basin (altogether data from 6 transects). Then, in each box, data are binned by month and year. For a given

month and box, the individual annual means are averaged for years 2001-2017. The seasonal cycle obtained is then further smoothed with a 1-2-1 smoothing average over successive months, as some of the calendar months were sampled in very few years (worse for the southern shelf box in January-May). Rms deviations of samples from this 'smoothed' seasonal cycle are largest during the periods with largest variability. Typically this happens in spring time (May-June) for parameters influenced by phytoplankton blooms. When presenting the average seasonal cycle (renormalized so that it corresponds to S=35, and for DIC and $\delta^{13}C$ with the trend added to correspond to 2010), we do not plot the uncertainty resulting from the sampling. This uncertainty which is difficult to estimate properly (as it is due both to interannual variability and variability within the same transect) is however usually much smaller than the seasonal cycle amplitude portrayed.

2.2.2 Estimating trends.

Trends are estimated separately from the seasonal cycle, although the two are intertwined due to the irregular time sampling. Earlier papers (Corbière et al., 2007; Metzl et al., 2010), mostly considered trends in winter. Here, trends are based either on all data or on data collected in one season (without removing the seasonal average). To minimize errors, either all data are considered, or only data in 50°N-63°N. Alternatively, the deviations from the average seasonal cycle are estimated in each box, but we will not discuss them further here. This is done for DIC, A_t, fCO_2, pH, and $\delta^{13}C_{DIC}$ and for different periods. Only the most characteristic trend estimates will be presented, for the sake of characterizing the dataset and comparing them with results of other products and analyses.

3 Seasonal cycle

In this section, we will present the average seasonal cycle portrayed in the 2001-2017 data. For T (not presented), one finds a seasonal cycle increasing from north to south, with amplitudes close to those portrayed in SST climatologies, such as HadSST3 (Kennedy et al., 2011). The seasonal cycle in S (Fig. 3) is also found as described at the surface in WOD13 (Boyer et al., 2013) with a maximum in February-May (February-April on shelf) followed by a gradual decline until a minimum in September (October, north of 62°N). The amplitude also increases from North to South.

The DIC seasonal cycle presents (Fig. 3) a maximum in March and a minimum in July (North) transitioning to August (south). The amplitude is maximum on the Newfoundland shelf (73 $\mu molkg^{-1}$), and north of 62°N (70 $\mu molkg^{-1}$) and is smallest for 58-62°N (48 $\mu molkg^{-1}$). There is a slight decrease

Earth Syst. Sci. Data Discuss., https://doi.org/10.5194/essd-2018-50
Manuscript under review for journal Earth Syst. Sci. Data
Discussion started: 24 April 2018

from March to April indicating the beginning of carbon consumption during blooms, and a very steep decline in April to May.

A_t (Fig. 3) has much smaller seasonal variability than DIC (here expressed as deviation from average relationship A_t-S), and estimated uncertainties of several μmol kg^{-1} are large compared with the seasonal cycle amplitude (uncertainties are larger on the shelf in January-May). After a minimum in February, there is a peak in April-June, with April in the interior and later months north of 62°N and on Newfoundland shelf, followed by a decrease until August north of 54°N (and later further south). The increase could be associated with late winter or early spring blooms reducing NO_3 and PO_4 for the formation of organic carbon, whereas the latter decrease could be associated with calcifying organisms such as coccolithophores, which are known to produce large late spring or early summer blooms in this part of the Atlantic, usually well past the large diatom-dominated blooms (Signorini et al., 2012)

The $\delta^{13}C_{DIC}$seasonal cycle (Fig. 3) updates Racapé et al. (2014), and provides further spatial resolution. It mirrors the cycle in DIC, with a maximum$\delta^{13}C_{DIC}$in July in the north shifting to August further south (and even early September on the shelf) (and increase of 0.7‰ or more compared to late winter). The increase is associated with production of organic matter and the associated fractionation, whereas the later decrease is associated with remineralisation and vertical mixing. Notice also a small spatial gradient in winter with increasing values from north to south (and decreasing salinity).

The three nutrients present a March maximum (like DIC) associated with maximum entrainment of subsurface water in the mixed layer, a slight decrease to April, and a later decrease until a July minimum for Si and an August minimum for PO_4 and NO_3. This shift in the cycle is also suggesting of a dominance of calcifying organisms in the later portion of the bloom, when Si levels have been strongly depressed. For PO_4 and NO_3there is a north to south decrease of the nutrients (but not so much for Si) in all seasons. The decrease is even stronger for NO_3 on the Newfoundland shelf, a sign of the contribution of fresher water from the Pacific Ocean and western Arctic having experienced denitrification on the shelves. Notice that summer NO_3 levels are very low in this average cycle south of 54°N. The seasonal cycle of the three nutrients corresponds roughly to climatologies that are available from WOD13, and also to the data of the time series station in the Irminger Sea close to Iceland (Olafsson et al., 2010).

$\delta^{18}O$ (and δD) present no significant seasonal deviations from their average relationship with S north of 58°N. At 54-58°N, there is an early winter minimum and a maximum in April-May, during a period with overall small salinity seasonal variability. South of 50°N, in the shelf region, one finds a late summer maximum as described near the shelf break in Benetti et al. (2016), where it was related to some extent to sea ice melt water. 50-54°N presents an intermediate situation between the seasonal cycles in these two regions with a spring to September maximum

Finally, the fCO_2 and pH seasonal cycles are estimated from monthly mean DIC and A_t in each box (Fig. 4) Here, we do it without normalizing to S=35, in order to compare fCO2, pH, DIC seasonal cycles with the climatology constructed by Takahashi et al (2014). Except for the southern region (46-50°N), fCO_2 presents a pronounced maximum in February – March associated with vertical mixing and entrainment of remineralized DIC in the surface layer and a minimum in June associated with the carbon use during the spring bloom. Similarly to DIC described above, the fCO_2 seasonality is most pronounced in the north (amplitude 90 µatm) and in the south (80 µatm from January to May), where the fCO_2 seasonal cycle exhibits secondary maximum (August) and minimum (November), as in the climatology. In the central regions (54-58°N and 58-62°N) the seasonal fCO_2 amplitude is on the order of 40 µatm and we estimate similar fCO_2 levels for each month in these two boxes, as was also found for DIC and nutrients (Fig 3). The oceanic fCO_2 are near (in December-March in the north) or well below the atmospheric level (Fig. 4a), the maximum ocean CO_2 sink being observed in the southern region in May (fCO_2^{ocean}-fCO_2^{atm} = -110µatm) a signal also picked up in climatology (Takahashi et al., 2009, 2014) and regularly observed in recent years during cruises conducted in May (5 cruises in 2004-2015, Wanninkhof and Pierrot, in Bakker et al., 2016). The pH seasonal cycle (Fig. 4b) mostly mirrors (with reverse sign) the seasonal cycle in fCO_2 (Fig. 4a), and its amplitude ranges between 0.04 (in the gyre) and more than 0.1 (in the south and north).

Examples of the comparison to the climatological seasonal cycle (Takahashi et al., 2014) are presented on Fig. 5. It shows the fCO_2, A_t, DIC and pH cycles for the two boxes in the central gyre (54-58°N and 58-62°N) where we observed homogeneous properties (Fig. 3). Recall that the climatology (Takahashi et al., 2014) for DIC and pH was calculated from pCO_2 and reconstructed alkalinity, and for reference year 2005, whereas our DIC seasonal cycle constructed with 2001-2017 data is referenced to year 2010 (section 2.2.a), and the corresponding fCO_2 and pH computed from this DIC and A_t. At 56°N (green lines), the fCO_2 (pH) climatology is low (high) compared to SURATLANT, but with rather similar seasonality. At 60°N (blue lines), fCO_2 and pH seasonality are stronger in the climatology with a more

Earth Syst. Sci. Data Discuss., https://doi.org/10.5194/essd-2018-50
Manuscript under review for journal Earth Syst. Sci. Data
Discussion started: 24 April 2018

pronounced fCO_2 minimum and pH maximum in June-July, but results are very similar in other seasons (August-May). For both regions, the A_t seasonal amplitude is most pronounced in the SURATLANT data (about 10-15 $\mu molkg^{-1}$, Fig 5b) with largest difference in August. Despite these differences, the DIC cycles derived from independent observations and methods are very similar (Fig 5c), which is typical of all the regions.

4. Trends

Although significant variations have been previously observed and discussed for some periods (e.g., a rapid ocean fCO_2 increase up to +7 $\mu atmyr^{-1}$in winter over 2001-2008, Metzl et al., 2010), here we show the trends over the full period (1993-2016) using all data or restricted to the band 50-63°N, and in summer (June-September) or winter (January-March). In this band, A_t does not show any trend (Fig.6), as well as salinity or nutrients (not shown). On the opposite, we find positive trends for DIC (~ +0.7 $\mu molkg^{-1}yr^{-1}$) in both summer and winter (notice no winter data included in 2016 or 2017) (Fig. 7). This trend is about half the one reported by Olafsson et al. (2009), based on winter observations in the Iceland Sea for years 1985-2008 (+1.4 $\mu molkg^{-1}$ yr^{-1}), but close to the trend observed over 1990-2015 in the Irminger Sea upper ocean waters (+0.63 $\mu molkg^{-1}$ yr^{-1}), a signal mainly explained by anthropogenic carbon uptake (Fröb et al., 2018b). As also suggested by $^{13}C_{DIC}$ data (described below), the positive DIC trends derived from SURATLANT data (Fig. 7) are likely due to anthropogenic CO_2. Also, interestingly, in both seasons, the SURATLANT data seem to present no trend before 2005, which corresponds to SST (and AMO) maximum. This lack of DIC trend in the early part of the record was also commented in Metzl et al. (2010). This first part of the record also corresponds usually to a period of decreasing winter winds (decrease in frequency of NAO+ situation), and thus an expected decrease in winter mixed layer depths (and also a decrease in subpolar gyre circulation).

For fCO_2 (derived here from At, DIC, SST…; cf 2.1) positive trends are found as expected (Fig.8). In the band 50-63°N, the summer (+2.1 μatm yr^{-1}) and winter (+1.67 $\mu atmyr^{-1}$) trends are close to the atmospheric increase. This is in the range of the long-term trend (25-30 years) estimated in the North Atlantic by Takahashi et al., (2009) and McKinley et al., (2011), but much lower than values near or above +3 μatm yr^{-1}previously reported for years 1993-2006 (Corbière et al., 2007; Schuster et al., 2009; Metzl et al., 2010) and much larger than the +1.1 $\mu atmyr^{-1}$trend estimated by Lauvset et al. (2015) for years 1991-2011 in the NASG. This highlights that fCO_2 trend is quite sensitive to the period (and data) selected (Fay and McKinley, 2013). Note that if one uses all data (all seasons and regions) the fCO_2 trend is +1.9 μatm yr^{-1}(Fig.9a) so that the delta-fCO_2 (difference between ocean and atmospheric

fugacities) present no significant trend (Fig. 9b) suggesting that in this region the air-sea CO_2 fluxes driven by delta-fCO_2 (and winds) are relatively constant over time. Although temperature interannual variations (up to +1.5 °C in 2005, or -1.5°C in 2015, cf Fig. B1) could explain rapid fCO_2 changes for some periods (Corbière et al. 2007), over the longer term the fCO_2 trends presented here are mainly explained by DIC (A_t being relatively constant). The same is true for pH (Fig.10) and its negative trend of -0.002yr^{-1} mirrors the fCO_2 trend. Similarly to fCO_2 trend, this pH trend for the NASG is close to the mean global ocean estimate of -0.0018yr^{-1}(Lauvset et al., 2015) and comparable to other trends evaluated in the North Atlantic polar waters, ranging between -0.0017 yr^{-1} and -0.0024 yr^{-1} depending on the periods, seasons and regions (Lauvset and Gruber, 2014; Lauvset et al., 2015; Olafsson et al., 2009).

For $\delta^{13}C_{DIC}$, we find significant trends in all seasons for the 2005-2017 period for which samples are available. The winter trend (-0.015‰yr^{-1}) is smaller than the summer trend (-0.042‰ yr^{-1}) (Fig. 11). Both are small compared to the seasonal cycle, and have large uncertainties, due to the small number of years sampled. Notice for example that the summer season is during a time of large seasonal change (Fig. 3). The trends seem of a similar magnitude since 2010, although in summer it is sensitive to the large positive deviations of August 2010 data (see Racapé et al., 2014), with lower trends in 2010-2017 when not including it (-0.0040 versus -0.042‰ yr^{-1}). However, the trend estimates are sensitive to uncertainties in the different corrections that we apply to the data before and after 2010 (see App. A3). Altogether, the surface winter trend deduced from the adjusted data set is lower than the expected Suess effect in the atmosphere (-0.025‰yr^{-1}, based on current change rates in atmospheric pCO_2, such as from the Alert station). It is also comparable with model estimates in the NASG for other periods from Sonnerup and Quay (2012; -0.12‰ $decade^{-1}$over the period 1970-95) and from Tagliabue and Bopp (2008; 0.10‰ $decade^{-1}$ between 1970 and 2005).

Data availability

The dataset is available at http://www.seanoe.org/data/00434/54517/

5. Conclusions

The SURATLANT data set in 1993-2017 is based mostly on discrete collection of surface samples (currently 2832 data points during 76 transects, but not always for all parameters). The collection methods and the parameters analysed have varied through the sampling, due to funding as well as logistical and analytical issues. We have documented data issues and have thus edited the data set. The

accuracy of the data is usually well documented (cf Annex A). Of course, we cannot guarantee that there are no remaining issue due for example to contamination of the water samples from pipes or water collection on board a ship, or due to storage in bottles before analysis in a laboratory. We derive a new A_t-S relationship adapted to the dataset that is used to estimate fCO_2 and pH, as well as other parameters of the carbonate systems, when A_t was not measured such as in 1993-1997. Thus estimated fCO_2 and pH are also provided with the dataset.

The sampling is found to be sufficient to document the average seasonal cycle of most parameters analysed in this region providing a coherent data-set for processes analyses and/or biogeochemical ocean models validation. It is also sufficient to document the long-term trends (1993-2017) in different seasons. These trend estimates are provided to illustrate properties of the data set, and are found to be in the bulk range of other studies. However, clearly, because of both interannual and decadal variability (for example indication of evolution that is different in the warming period until 2005 than afterwards), it is rather difficult to compare with other analyses, without further information on the variability, either from other datasets or model simulations. Furthermore, the possibility of large spatial variability in these signals could complicate the comparison. For example, Fröb et al. (2018a) document a large spatial change in the recent decrease of SSS across the Reykjanes Ridge that implies (based on fCO_2 observations) different decadal trends in DIC between the two regions.

In addition to this data set of discrete samples, other measurements have been made on the same ships of opportunity throughout most of the 24 years of operation by continuous measurements. These include near surface temperature and salinity from TSGs, and also at times pCO_2 measured with equilibrator systems. Notice also that the information on instantaneous mixed layer depth and stratification information was provided in a large part of the time by XBT profiles. These different data sets (operated by NOAA/AOML and LOCEAN) will have to be incorporated to provide further analysis of the discrete water samples. Validated versions of these complementary datasets can be downloaded from the different sites mentioned in the paper. The investigation should also be based on the compilations of stations data in GLODAP (Olsen et al., 2016) or the very rich SOCAT (Bakker et al., 2016) data base. There is also a large array of complementary observations, such as from the Argo and the bio-Argo (Organelli et al., 2017) data sets. For example, these data suggest blooms in mid-winter that could have a depletion impact on net production and export of nutrient and carbon from the surface layer already in March (Lacour et al., 2017). Notice however that the bio-Argo floats have mostly sampled the rim of the subpolar gyre and provide only indirect evidence on near-surface carbon

and nutrient that they did not measure. Thus combining the different in situ cruise data sets with the Argo data will provide other challenges.

Earth Syst. Sci. Data Discuss., https://doi.org/10.5194/essd-2018-50
Manuscript under review for journal Earth Syst. Sci. Data
Discussion started: 24 April 2018

405
406 **Appendix A**: **Data methods and uncertainties**

407 We will review the different chemical parameters analysed, and discuss the uncertainties, as well as
408 anomalies observed.

409

410 **A.1 Inorganic macro-nutrient (nitrate, phosphate, silicic acid) concentrations:**

411 Samples for macro-nutrient concentrations were collected starting in late 2001 in pre-cleaned 250 ml
412 low density polyethylene bottles that were frozen on board (for two crossings, the samples were
413 probably not correctly frozen, and are discarded). For spring and summer samples, filtering was done
414 before measuring the macro-nutrient concentrations of nitrate (including nitrite), phosphate and silicate.
415 They were measured usually within 3 months of collection with standard colorimetric methods at the
416 Marine Research Institute (Reykjavik, Iceland). The analytical procedure and the quality control for
417 the nutrient analyses have been described in detail in Olafsson et al. (2010) where the long term
418 accuracy has been estimated as ±0.2 µmol kg^{-1} for nitrate (includes also nitrite) and silicate, and ±0.03
419 µmol kg^{-1} for phosphate. Additional uncertainties could result from contamination during collection, or
420 from poor conservation of the nutrients in the frozen samples. In particular this can result in occasional
421 elevated levels in phosphate, which are discarded when too far from neighboring samples with similar
422 T, S and DIC, or from the expected largest values. Values of phosphate were deemed too low in
423 January 2017, when it was found that most of the water had gone through some storage resulting into a
424 too large contribution of particulate phosphate to total inorganic phosphate.

425

426 Samples for phosphate in 1993-1994 were poisoned and analyzed at LDEO (Columbia Univ., New
427 York) shortly after the return of the water samples. Samples during RREX2017 (July/August 2017)
428 were pasteurized, kept cool and analyzed 5 months after the cruise at UMS IMAGO of IRD in Brest.
429 Samples from these different laboratories have not been inter-compared, and are reported as such.

430

431 **A.2 Dissolved inorganic carbon and total alkalinity**

432 Since June 2001, water samples collected on the ship are then shipped back to LOCEAN (Paris) where
433 they are stored at 4°C and analyzed within three months of collection. No filtration is done, thus there
434 might be a small amount of particulate inorganic carbon measured as well. DIC is determined at the
435 same time as total alkalinity (A_t) by potentiometric titration derived from the method developed by
436 Edmond (1970) using a closed cell and calibrated Certified Reference Material (CRM) provided by A.
437 Dickson (Scripps Institution of Oceanography, San Diego, USA). Analytical accuracy of the DIC and

438 At concentrations is ±3 µmol kg^{-1} (further details in Corbière et al. (2007)). Most of the bottles used at
439 LOCEAN since 2003 were 500 ml round bottles with screw caps (before that and for a few isolated
440 samples since 2003, the 500 ml bottles had a ground glass stopper and Apiezon grease was used). For
441 some of these bottles, we found that samples presented systematic biases in 2010-2015, either in DIC
442 or A_t. This led to the replacement of some bottles in July 2015, and after that, most bottles are from a
443 newer set. Since 2005, poison (saturated (or half saturated) mercuric chloride solution) volumes were
444 kept to 0.3 ml, and no correction was applied for dilution. In earlier years, poison solution volume has
445 evolved, and data reported are usually corrected for the dilution effect. For the period 06/1993-02/1997,
446 the samples were stored in bottles with ground glass stopper with use of Apiezon grease, and DIC was
447 determined by a coulometric method at LDEO (Chipman et al., 1993). For some samples in 2005-2006
448 associated with a $\delta^{13}C_{DIC}$value, DIC was also estimated manometrically during acid CO_2 extraction
449 procedure with somewhat lesser accuracy (±5 µmol kg^{-1}). We used these DIC values when there was
450 no DIC estimated at LOCEAN.
451
452 We first edited the data to remove suspicious values. In particular, in some instances, errors seemed to
453 have resulted from poor sample conservation in the bottles before analysis. For example, we often
454 noticed erroneously large DIC and A_t values from bottles 8 (103-mid 2015) and 19 (08/2010 to mid-
455 2015). There are also a few transects when samples had to be discounted. In one case (April 2007) this
456 happened because the samples were stored in a very hot space before shipment to France. For April
457 2015 DIC values were too high for unknown reasons (but possibly, the bottles had aged), and for
458 January 2017, both DIC and A_t were discounted as the origin of the water collected was suspicious
459 (problem also encountered for salinity samples and with the phosphate, with an anomalous contribution
460 of particulate phosphate). In April 2015, we adjusted the DIC values by -10.3 µmol kg^{-1}, based on
461 comparisons of estimated fCO_2 with those directly measured that are in the AOML and SOCAT data
462 base.
463
464 The LOCEAN DIC values have been compared for some crossings with DIC samples collected at the
465 same time and analyzed in other laboratories(in 2005, 2006, 2010, 2015, 2016 and 2017, that altogether
466 involved four laboratories). These comparisons summarized in Table A1 (average and rms standard
467 deviation)reveal for individual transects LOCEAN DIC often lower by 5 µmol kg^{-1} or more, but this is
468 far from being systematic. Very often, dilution by the mercury chloride solution is taken into account
469 by other groups, but not at LOCEAN, which could contribute to up to 2 µmol kg^{-1} difference
470 (LOCEAN DIC lower).There can also be issues of poor conservation of some of the other water

samples and uncertainties in their analysis, so this is not an absolute validation of the LOCEAN values. Usually, the comparisons for A_t (in 2010, 2015 and 2016) suggest smaller average differences. For A_t there were other comparisons of samples collected in the same region and analyzed both at LOCEAN and ICM/CSIC during the Ovide cruises (every 2 years between 2002 and 2016) but with a different set of LOCEAN bottles than for SURATLANT. They suggest a similarly close agreement between A_t analyzed in the two laboratories (for example, average difference of -1.4 (σ=3.4 n=57) µmol kg^{-1} for the 2014 cruise). A recent international inter-comparison on two shared water batches (spring 2017) suggests that the LOCEAN analysis presents a small negative bias both for A_t and DIC, but not in a very similar range of values to the ones observed during SURATLANT.

Whether these results are relevant for the whole dataset will need to be further ascertained. We can nonetheless expect that the DIC and A_t reported in the SURATLANT data set have uncertainties always smaller than 10 µmol kg^{-1}, that they can present biases at time, but that they are probably of a higher accuracy most of the time. To provide further validation, we take advantage that during some transects, sea surface underway fCO2 measurements were also conducted following Pierrot et al., (2009) and data available at AOML (http://www.aoml.noaa.gov/ocd/ocdweb/occ.html) and regularly submitted and qualified in SOCAT (Bakker et al, 2016). We have collocated these data (within 2 minutes time of discrete sampling) and compared them with fCO2 calculated from DIC, At pairs. For this comparison we only use samples when DIC and At were measured (not At derived from salinity if At is missing). A total of 172 points have been collocated for different years (2004-2007 and 2014-2015), for almost all seasons (months: Jan, Feb, Apr, Jun, Jul, Oct, Nov and Dec) and those data represent a large fCO2 range (225-420 µatm, Figure A1a). We find both positive and negative differences (Figure A1b) that are not associated to years, seasons, SST, DIC or At concentrations. The mean difference (fCO2calc-fCO2mes) of -3.6 (+/- 12.4) µatm is thus attributed to methods uncertainties (including sampling time, measurements errors and data processing). These new results (mean and deviation) are in the same range as obtained in previous comparisons (Metzl et al., 2010) but for different, fewer data and different constants (n=54, mean difference= -2.3 (+/- 11.1) µatm). We thus conclude that fCO2 (and pH) calculated here with discrete DIC, At data are suitable to interpret both seasonality and trends.

A.3 $\delta^{13}C_{DIC}$:

Over the period 2005-06, acid CO_2 extraction was done for $\delta^{13}C_{DIC}$ measurements from helium

stripping technique. This analytical method has been described previously by Quay and Stutsman (2003). These measurements have an accuracy of ±0.02‰ for $\delta^{13}C_{DIC}$ based on a helium stripping technique adapted from the one used by Kroopnick (1974) and ±5µmol kg^{-1} for DIC based on a comparison to coulometric DIC values and to Certified Reference Material (CRM) provided by A. Dickson (Scripps Institution of Oceanography, San Diego, USA). However, the DIC of these samples were higher by an average 5 µmolkg^{-1}than the LOCEAN DIC. If this was caused by a small remineralization of dissolved organic DIC, and based on the relationship described in Racapé et al (2014), this could be associated with a negative bias of -0.05‰ in $\delta^{13}C_{DIC}$.Thus, we chose to correct these pre-2006 data by 0.05‰.

Over the period 2010-17 during most of the SURATLANT cruises, $\delta^{13}C_{DIC}$ were measured by mass spectrometry via an acid CO_2 extraction method in a vacuum system developed by Kroopnick (1974) whereas further details on the sampling methods and analytical techniques are provided in Racapé et al. (2014) for $\delta^{13}C_{DIC}$. Water was collected in small glass bottles poisoned by at least 1 ml of saturated solution of mercuric chloride, and stored in the dark when possible at 4°C (at least, after return to the lab, when it was stored for up to a year before analysis). Data of some crossings were dismissed, probably because poisoning had been insufficient, and for one crossing the mass spectrometer did not function properly. Other isolated samples were dismissed either because not enough gas was collected after acidification or due to possible leaks on the mass spectrometer gas lines. These $\delta^{13}C_{DIC}$ values are expected to have a precision of ±0.01‰ (Vangriesheim et al., 2009) and a reproducibility of ±0.02‰. Issues on the accuracy of other $\delta^{13}C_{DIC}$samples from LOCEAN have been raised, and LOCEAN participated to an inter-laboratory comparison run by C. Normandeau (Dalhousie University) with deep NASG water samples conditioned by Dahlousie Univ. The results suggest that recent LOCEAN samples have a slightly poorer reproducibility (±0.04‰) than earlier ones. These comparisons suggest an average bias of LOCEAN measurements of -0.13‰. This is less than the -0.25‰ (0.20 to 0.30‰) bias corrected in the GLODAP database to LOCEAN samples collected during North Atlantic cruises in 2002 and 2006and analyzed with the same method and standards as here. This adjustment was based on the intercomparison of different cruises (Becker et al., 2016), which could nonetheless include a part due to anthropogenic signal. We chose to adjustall the LOCEAN values (samples collected in 2010-2017) by +0.13‰.

A.4 Water isotopologs:

Since 12/2011, the oxygen isotopic composition of discrete sea water samples has been usually

analyzed with a PICARRO CRDS (cavity ring-down spectrometer; model L2130-I Isotopic H_2O) at LOCEAN-IPSL (Paris, France). The internal referenceswhich have been used to calibrate the data in the V-SMOW scale, have been previously calibrated using IAEA references and vary from -6.61‰ to 2.24 ‰ for $\delta^{18}O$ and from -44.3 ‰ to 3.31 ‰ for δD.All reference watersare stored in steel bottles with a slight overpressure of dry nitrogen to avoid evaporation processes and exchanges with ambient air humidity. Based on repeated analyses of an internal laboratory standard over several months, the accuracy of the measurements is usually better than ± 0.05 ‰ for $\delta^{18}O$ and ± 0.50 ‰ for δD. All sea water samples before 04/2016 have been distilled to avoid salt accumulation in the vaporizer and its potential effect on the measurements (e.g., Skrzypek and Ford, 2014). Between 04/2016 and 07/2016, as well as since May 2017, the analysis has been often done without distillation and with a salt trap mesh. Samples in 09-10/2016, 01/2017, as well as a few samples in05/2017 and 08/2017 samples were instead analyzed on a GV Instruments Isoprime dual inlet IRMS coupled with Aquaprep sample preparation system (at IES, Reykjavik, Iceland). The different methods are fully described in Benetti et al. (2017).All samples in 1993-1995 were analyzed on a similar Isoprime dual inlet IRMS system but at LDEO. Most of the samples done on IRMS were only run for$\delta^{18}O$. A recent study (Benetti et al., 2017) suggests that different corrections have to be applied on the data depending on the method used to report the data in 'absolute concentration scale'. We follow their recommendations and adjusted data to 'absolute concentration scale', except for the following cases. For the $\delta^{18}O$ values of samples in 1993-1995, for which the information on the internal standard used has been lost (although it probably was deep Atlantic Ocean water), we assume that they are already reported in concentration scale, and apply no correction. For the 12/2011 section, samples were analyzed either by the PICARRO CRDS (but without distillation), or at LOCEAN with a GV Instruments Isoprime dual inlet IRMS coupled with Aquaprep sample preparation system (with$\delta^{18}O$ adjusted to the PICARRO measurements), and the accuracy of these samples is not as high (probably closer to ± 0.10 ‰ for $\delta^{18}O$ and ± 1.00 ‰ for δD). Finally, for data of a 2017 run with a different salt trap mesh, we found a slight additional bias that was also corrected.

Earth Syst. Sci. Data Discuss., https://doi.org/10.5194/essd-2018-50
Manuscript under review for journal Earth Syst. Sci. Data
Discussion started: 24 April 2018

565 **Appendix B: A_t-S relationship and resulting uncertainties in estimating fCO_2 and pH**

566 As explained in 2.1, we constructed anA_t-S linearrelationship by least square fitting on the
567 SURATLANT data (2001-2016) for S larger than 34, mixing all seasons. The R^2 correlation coefficient
568 is 0.83 and rms deviations of 8.4 μmol kg^{-1} (for S larger than 34), which is larger than the uncertainty
569 on the measurements. We also suggested when describing the seasonal cycle of A_t in section 3 that part
570 of the scatter could be due to seasonal variability, and certainly there is a range of variation expected
571 for this relationship. Here, we will document what effect the choice made has when estimating fCO_2 or
572 pH from DIC, SSS, SST, nutrient data, when A_t was not measured such as in 1993-1997. In particular,
573 it is interesting to estimate how it affects trends, as done in section 4.
574
575 First, we compare the computed versus measured A_t (Fig. B1). They present differences that tend to be
576 correlated over a year or more, such as the lower computed values in 2001-early 2005, 2011-2012 or
577 part of 2015. On the other hand there is no significant trend in the difference between the two during
578 the measurement period from 2001 to 2017. Not surprisingly, the same can be said for computed fCO_2
579 or pH (Fig. B1). Therefore the conclusions on the long-term trend for fCO_2 and pH are valid using A_t,
580 either from measurements or A_t/S relation, but for short-term and processes analyses measured A_t
581 should be used.
582
583 We then compare the alkalinity estimated with the SURATLANT relationship with the one derived
584 with the relationship by Nondal et al (2009) which has a steeper slope. We also show the earlier fit of
585 Corbière et al (2007), which result in larger A_t, and a fit on all the SURATLANT data, including the
586 shelf data for S< 34 (Fig. B2). The Nondal et al (2009) relation underestimates A_t for low S, but is
587 rather well within the data spread near S=34 – 35 psu. The Corbière et al. (2007) relationship
588 overestimates A_t at all salinities, and will not be considered later on.
589
590 We then compare $fCO_2$and pH computed with the two best estimated A_t(S) which seem to cover the
591 possible range of relationships. When applied on all the individual data, the difference (fCO_2 using the
592 SURATLANT relationship minus fCO_2 using the Nondal et al (2009) relationship) appears as a spread
593 for S near 35, as well as for the low S on the shelves (Fig. B3). For all samples for S>34, the mean
594 difference is 3.8 (+/- 1.75) μatm, i.e. lower than uncertainty associated to fCO2 calculations. As overall
595 changes in S are not that large over the 24 years (cf App. C) these two At/S relations, originally based
596 on different data-sets, lead to same conclusion for the fCO_2 trend (1.7-1.8 μatm yr^{-1}) that is close to the

Earth Syst. Sci. Data Discuss., https://doi.org/10.5194/essd-2018-50
Manuscript under review for journal Earth Syst. Sci. Data
Discussion started: 24 April 2018

597 trend in the atmosphere. The impact on the trend in pH is also not significant.

598

599

600

Earth Syst. Sci. Data Discuss., https://doi.org/10.5194/essd-2018-50
Manuscript under review for journal Earth Syst. Sci. Data
Discussion started: 24 April 2018

Appendix C: T and S time series in the subpolar gyre

We also estimated monthly binned temperature and salinity time series (smoothed 1-2-1 over successive months) along a standard ship route since mid-1993 (B-AX02 transect between Iceland and southern Newfoundland) which is close to where most samples were collected (Fig. 1). Most data originate from ship-mounted thermosalinographs with additional data from XBTs, CTDs, instrumented drifters and floats (Argo floats or the earlier Palace floats). The data qualification, processing and how the gridded time series are produced, is reported in Reverdin et al. (2018). To summarize the main steps: an average seasonal cycle at 1° resolution is first removed from individual data, and anomalies are then grouped in bins along the ship track on a monthly time scale. Gaps in the time series are filled by first linearly interpolating from neighbouring spatial bins, and then in time from neighbouring time steps (with a further 1-2-1 running average on the monthly anomaly time series). Time series along the AX02 transect start in July 1993 with monthly few short gaps (the largest gaps are found in winter over the Newfoundland shelf and slope). These time series are used to check whether the discrete sampling presented in this paper has accounted for the interannual/decadal variability portrayed in this time series. They are also helpful in estimating the domains over which the hydrographic variability presents some coherence.

Hovmüller diagrams of T and S along AX02 are presented on Fig.C1 (left panels). Along this transect, bins correspond usually to 1° latitude range, with two wider bins on the shelf between southern Newfoundland and the shelf break, and two bins that correspond to the Newfoundland shelf break and slope. The T and S AX02 time series usually present large correlation between successive seasons (correlation coefficient higher than 0.6), except for the two time series on the Newfoundland shelf. The S variability along AX02 is very coherent in latitude from the close vicinity of Iceland to 54°N, and after a strong increase in 1996 present oscillations at 4-10 years period, before a recent decrease in 2016-2017. The transition at 54°N corresponds to North Atlantic Current frontal position further east and where the line stops paralleling the western flank of the Reykjanes Ridge. Further south over the deep ocean (until 49°N/49°W), variability in S is much larger, but not similarly phased to what is observed further north, with some suggestion of a lead-time of one to two years. Variability is different on the Newfoundland shelf and less coherent between successive seasons. The data sampling there is not always sufficient to be correctly portrayed in this analysis, in particular due to occasional winter or early spring ice cover, in particular in 1994-1995 and in 2014-2016. Still, it seems also to indicate negative low frequency anomalies until 2000 and between 2010 and 2015, and more positive in between, as is found further offshore.

634

635 T is not well correlated to S, in particular at seasonal to interannual periods, but the time series are too
636 short to identify whether correlation increases at lower frequencies. There is a large meridional
637 coherency in the signals at least north of 50°N. This clearly resembles the subpolar gyre scale AMO
638 index or average temperature, such as presented for example in Robson et al. (2016). There is the clear
639 swing from negative T-anomalies before 1996, and again in 2000, to maximum positive anomalies in
640 2004-2007 or 2010, followed by more negative anomalies (as seen in Robson et al., 2016) that have
641 amplified in 2014-2016.

642

643 We compared the winter S anomalies from the binned analysis (B-AX02) with the deviations from the
644 average seasonal cycle from the discrete water samples of the SURATLANT data set. The comparison
645 is very encouraging, as illustrated by the salinity plots at 60°N (Fig. C2). Clearly the SURATLANT
646 reduced sampling is able to capture the largest signals in salinity (and in temperature) and thus in
647 surface water masses, that the ocean witnessed. This holds also to a good extent in other seasons, and
648 less so on the Newfoundland shelf, where variability tends to be more high frequency. Notice though
649 that there are inter-annual differences. For example, SURATLANT would describe (at this latitude),
650 early 1997 as anomalously fresh, whereas B-AX02 shows near-normal salinity conditions.

651
652

653
654 **Author contribution**
655 GR has remained the prime coordinator of the project since it was initiated in 1993 and prepared the
656 manuscript with contributions from all co-authors. NM has been co-Pi on most of the proposals since
657 2000 and has contributed to the collection, qualification and validation of large parts of the data set. SO
658 has been in charge of the nutrients since 2001 as well as intercomparison of DIC/A_t samples, and is the
659 main Icelandic PI associated to the project. VR has been in charge of the validation of the $\delta^{13}C_{DIC}$ data.
660 TT has contributed to the initiation of the project in 1993, and has produced the DIC and PO_4 data
661 before 1997. MB has been in charge of the validation of the water stable isotope data. HV has been
662 associated in Iceland to the initiation of the project and has supervised the analysis of salinity samples
663 since 2000. ABC has performed the analysis of nutrient data since 2010. MD has analyzed the salinity
664 samples since 2001. JF has performed and qualified the DIC/A_t analyses since 2014. AN has analyzed
665 many $\delta^{13}C_{DIC}$ and water stable isotope samples.
666
667 **Acknowledgments**

668 The authors declare that they have no conflict of interest. Access on the merchant vessels run or leased
669 by EIMSKIP has been the core for this long effort to maintain surface sampling between Iceland and
670 Newfoundland. The nearly one hundred volunteer ship riders and their enthusiasm have been key to the
671 success of this monitoring. The project was initiated when one of the authors, GR, was at LDEO, with
672 initial support from this institution. NOAA/AOML and NOAA/CPO Ocean Observing and Monitoring
673 Division have contributed by maintaining the thermosalinographs and providing XBTs on the different
674 ships that have operated between Iceland and Newfoundland. The French effort was supported by
675 various agencies throughout the years, and in particular INSU (for SNO SSS and by the LEFE/CYBER
676 grant CO2SINK since 2016). Support by National Power Company of Iceland Landsvirkjun is
677 acknowledged.The $\delta^{13}C_{DIC}$ sampling was initiated by Paul Quay (Univ. of Washington, Seattle) in
678 2005-2006. SNAPO-CO2 is acknowledged for analyzing DIC/A_t at LODYC/LOCEAN since 2001, and
679 the isotopic platform of OSU Ecce Terra for analyzing $\delta^{13}C_{DIC}$ as well as water stable isotopes at
680 LOCEAN since 2010. Collaboration between French and Icelandic investigators has been supported by
681 PHC Jules Verne 2016 grant 36187YF. Support to Virginie Racapé (most recently by IFREMER) and
682 Marion Benetti (grant from the University of Iceland in Reykjavik). The very supportive help of
683 Christian Brunet for the analysis of DIC/A_t samples in 2001-2014 is also warmly acknowledged.
684 Support from the European Integrated Project CARBOOCEAN (511176) is also acknowledged
685
686 We have not identified competing interests
687

688
689 **References**

690 Alory, G., Delcroix, T., Téchiné, P., Diverrès, D., Varillon, D., Cravatte, S., Gouriou, Y., Grelet, J.,
691 Jacquin, S., Kestenare, E., Maes, C., Morrow, R., Perrier, J., Reverdin, G., and Roubaud, F.:The
692 French contribution to the voluntary observing ships network of sea surface salinity, Deep Sea Res. I,
693 105, 1–18, doi:http://dx.doi.org/10.1016/j.dsr.2015.08.005, 2015.
694
695 Antonov, J. I., Seidov, D., Boyer, T. P.,Locarnini, R. A., Mishonov, A. V., Garcia, H. E., Baranova, O.
696 K., Zweng, M. M., and D. R. Johnson, D. E.: World Ocean Atlas 2009, Volume 2: Salinity. S. Levitus,
697 Ed. NOAA Atlas NESDIS 69, U.S. Government Printing Office, Washington, D.C., 184 pp, 2010.
698
699 Bakker, D. C. E., Pfeil, B., Landa, C. S., Metzl, N., O'Brien, K. M., Olsen, A., Smith, K., Cosca, C.,
700 Harasawa, S., Jones, S. D., Nakaoka, S.-I., Nojiri, Y., Schuster, U., Steinhoff, T., Sweeney, C.,
701 Takahashi, T., Tilbrook, B., Wada, C., Wanninkhof, R., Alin, S. R., Balestrini, C. F., Barbero, L.,
702 Bates, N. R., Bianchi, A. A., Bonou, F., Boutin, J., Bozec, Y., Burger, E. F., Cai, W.-J., Castle, R. D.,
703 Chen, L., Chierici, M., Currie, K., Evans, W., Featherstone, C., Feely, R. A., Fransson, A., Goyet, C.,
704 Greenwood, N., Gregor, L., Hankin, S., Hardman-Mountford, N. J., Harlay, J., Hauck, J., Hoppema,
705 M., Humphreys, M. P., Hunt, C. W., Huss, B., Ibánhez, J. S. P., Johannessen, T., Keeling, R., Kitidis,
706 V., Körtzinger, A., Kozyr, A., Krasakopoulou, E., Kuwata, A., Landschützer, P., Lauvset, S. K.,
707 Lefèvre, N., Lo Monaco, C., Manke, A., Mathis, J. T., Merlivat, L., Millero, F. J., Monteiro, P. M. S.,
708 Munro, D. R., Murata, A., Newberger, T., Omar, A. M., Ono, T., Paterson, K., Pearce, D., Pierrot, D.,
709 Robbins, L. L., Saito, S., Salisbury, J., Schlitzer, R., Schneider, B., Schweitzer, R., Sieger, R.,
710 Skjelvan, I., Sullivan, K. F., Sutherland, S. C., Sutton, A. J., Tadokoro, K., Telszewski, M., Tuma, M.,
711 Van Heuven, S. M. A. C., Vandemark, D., Ward, B., Watson, A. J., and Xu, S.: A multi-decade record
712 of high-quality fCO_2 data in version 3 of the Surface Ocean CO_2 Atlas (SOCAT), Earth Syst. Sci. Data,
713 8, 383-413, doi:10.5194/essd-8-383-2016, 2016
714
715 Becker, M., Andersen, N., Erleukeuser, H., Humphreys, M. P., Tanhua, T., and Körzinger, A.: An
716 internally consistent dataset of d13C-DIC in the North Atlantic Ocean – NAC13v1. Earth Sys. Sci.
717 Data, 8, 559-570, doi:10.5194/essd-8-559-2016, 2016.
718
719 Benetti, M., Reverdin, G., Pierre, C., Khatiwala, S., Tournadre, B., Olafsdottir, S., and Naamar, A.:
720 Variability of sea ice melt and meteoric water input in the surface Labrador Current off Newfoundland.
721 J. Geophys. Res. Oceans, 121, 2841–2855, doi:10.1002/2015JC011302, 2016.
722
723 Benetti, M., Sveinsbjörnsdottir, A. E.,Olafsdottir, R., Leng, M. J., Arrowsmith, C., Debondt, K.,
724 Fripiat, F., and Aloisi, G.: Inter-comparison of salt effect correction for $\delta^{18}O$ and $\delta^{2}H$ measurements in
725 seawater by CRDS and IRMS using the gas-G2O equilibration method. Mar. Chem.,194, 114-123,
726 2017.
727
728 Boyer, T.P., Antonov, J. I., Baranova, O. K., Coleman, C., Garcia, H. E., Grodsky, A., Johnson, D. R.,
729 Locarnini, R. A., Mishonov, A. V., O'Brien, T. D., Paver, C. R., Reagan, J. R., Seidov, D., Smolyar,
730 and I. V., Zweng, M. M.: World Ocean Database 2013, NOAA Atlas NESDIS 72, S. Levitus, Ed.,
731 Mishonov, A., Technical Ed.; Silver Spring, MD, 209 pp, 2013.
732
733 Boyer, T.P., Levitus, S., Antonov, J., Locarini, R., Mishonov, A., Garcia, H., and Josey, S.A.: Changes
734 in freshwater content in the North Atlantic Ocean 1955-2006. Geophys. Res. Lett., 34,
735 doi:10.1029/2007GL030126, 2007.

Chafik, L., Häkkinen, S., England, M. H., Carton, J. A., Nigam, S., Ruiz-Barradas, A., Hannachi, A., and Miller, L.:Global linkages originating from decadal oceanic variability in the subpolar North Atlantic, Geophys. Res. Lett., 43(20), 10,909–10,919, doi:10.1002/2016GL071134, 2016GL071134, 2016.

Chipman, D. W., Marra, J. and Takahashi, T.: Primary production at 47N and 20W in the North Atlantic Ocean: a comparison between the 14C incubation method and the mixed layer carbon budget. Deep-Sea. Res. 40(1/2), 151–169, 1993.

Corbière, A., Metzl, N., Reverdin, G., Brunet, C., and Takahashi, T.: Interannual and decadal variability of the oceanic carbon sink in the North Atlantic subpolar gyre. Tellus B, 59, 2, 168-178, doi :10.1111/j.1600-0889.2006.00232.x, 2007.

Daniault, N., Mercier, H.,Lherminier, P.,Sarafanov, A., Falina,A., Zunino, P.,Pérez, F. F., Rios, A. F.,Ferron, B., Huck, T., Thierry, V., and Gladyshev, S.:The northern North Atlantic Ocean mean circulation in the early 21st Century, Prog. Oceanogr. , 146, 142-158, doi:10.1016/j.pocean.2016.06.007, 2016.

De Jong, M.F., and de Steur, L.: Strong winter coolingover the Irminger Sea in winter 2014-2015, exceptional deep convection, and the emergence of anomalously low SST. Geophys. Res. Lett., 43, 7106-7113, doi:10.1002/2016GL069596, 2016.

Edmond, J. M.: High precision determination of titration alkalinity and total carbon dioxide content of sea water by potentiometric titration. Deep-Sea Res. 17, 737–750, 1970.

Fay, A. R., and McKinley, G. A.: Global trends in surface ocean pCO2from in situ data, Global Biogeochem. Cycles, 27, doi:10.1002/gbc.20051, 2013.

Frajka-Williams, E., Beaulieu, C., and Duchez, A.: Emerging negative Atlantic Multidecadal Oscillation index in spite of warm subtropics, *Scientific Reports* **7**, 11224, doi:10.1038/s41598-017-11046-x, 2017.

Friedman, A.R., Reverdin, G., Khodri, M. and Gastineau, G.:A new record of Atlantic sea surface salinity from 1896 to 2013 reveals the signatures of climate variability and long-term trends. Geophys. Res. Lett., 44, 1866–1876, DOI:10.1002/2017GL072582, 2017.

Friis, K., Körtzinger, A., and Wallace, D. W. R.: The salinity normalization of marine inorganic carbon chemistry data, Geophys. Res. Lett., 30(2), n/a–n/a, doi:10.1029/2002GL015898, 1085, 2003.

Fröb, F., Olsen, A., Becker, M., Chafik, L., Johannesen, T., Reverdin, G., and Omar, A.: Impact of recent North Atlantic freshening and cooling on the carbon cycle. Geophys. Res. Lett., in review, 2018a.

Fröb, F., Olsen, A., Pérez, F. F., García-Ibáñez, M. I., Jeansson, E., Omar, A., and Lauvset, S. K.: Inorganic carbon and water masses in the Irminger Sea since 1991, Biogeosciences, 15, 51-72, https://doi.org/10.5194/bg-15-51-2018, 2018b.

Fröb, F., Olsen, A., Våge, K., Moore, K., Yashayaev, I., Jeansson,E., and Rajasakaren, B.: Irminger Sea deep convection injects oxygen and anthropogenic carbon to the ocean interior, Nature Communications, 7, 13 244, doi:10.1038/ncomms13244, 2016.

García-Ibáñez, M. I., Zunino, P., Fröb, F., Carracedo, L. I., Ríos, A. F., Mercier, H., Olsen, A., and Pérez, F. F.:Ocean acidification in the subpolar North Atlantic: rates and mechanisms controlling pH changes, Biogeosciences, 13, 3701-3715, https://doi.org/10.5194/bg-13-3701-2016, 2016.

Gattuso, J.-P., and Hansson, L.:*Ocean Acidification*, Oxford University Press, New York, 2011.

Good, S. A., Martin, M. J., and Rayner, N. A.: En4: quality controlled ocean temperature and salinity profiles and monthly objective analyses with uncertainty estimates, J. Geophys. Res., 118, 6704–6716, doi:10.1002/2013JC009067, 2013.

Gruber, N., Keeling, C. D., Bacastow, R. B., Guenther, P. R., Lueker, T. J., Whalen, M., Meijer, H. A. J., Mook, W. G., and Stocker, T. F.: Spatiotemporal patterns of carbon-13 in the global surface oceans and the oceanic Suess effect, Global Biogeochem. Cy., 13, 307–335, 1999.

Häkkinen S., and Rhines, P. B.:Atmospheric blocking and Atlantic multidecadal ocean variability, Science, 334(6056), 655–659, doi:10.1126/science.1205683, 2004.

Häkkinen S., Rhines, P. B., and Worthen, D. L.:Atmospheric blocking and Atlantic multidecadal ocean variability, Science, 334(6056), 655–659, doi:10.1126/science.1205683, 2011.

Hátún, H., Sando, A. B., Drange, H., Hansen, B., and Valdimarsson, H.: Influence of the Atlantic subpolar gyre on the thermohaline circulation. Science 309,1841-1844, 2005.

Kennedy, J. J., Rayner, N. A., Smith, R. O., Parker, D. E., and Saunby, M.: "Reassessing Biases and Other Uncertainties in Sea Surface Temperature Observations Measured in Situ since 1850: 1. Measurement and Sampling Uncertainties." Journal of Geophysical Research 116 (July 22, 2011): 13 pp. doi:201110.1029/2010JD015218, 2011.

Khatiwala, S., Tanhua, T., Mikaloff, T., Fletcher, S., Gerber, M., Doney, S. C., Graven, H. D., Gruber, N., McKinley, G. A., Murata, A., Ríos, A. F. and Sabine, C. L.: Global ocean storage of anthropogenic carbon, Biogeosciences, 10, 2169-2191, https://doi.org/10.5194/bg-10-2169-2013, 2013.

Kroopnick, P.:Correlations between 13C and ΣCO2 in surface waters and atmospheric CO2:Earth and Planet. Sc. Lett. 22, 397-403, 1974.

Lacour, L., Ardyna, M., Stec, K. F., Claustre, H., Prieur, L., Poteau, A., D'Alcala, M. R., Iudicone, D.: Unexpected winter phytoplankton blooms in the North Atlantic subpolar gyre. *Nature Geoscience* 10: 836-839 | DOI: 10.1038/ngeo3035, 2017.

Landschützer P., Gruber, N., and Bakker, D.:Decadal variations and trends of the global ocean carbon sink, Global Biogeochem. Cycles, 30, doi:10.1002/2015GB005359, 2016.

Lauvset, S. K., and Gruber, N.: Long-term trends in surface ocean pH in the North Atlantic, Mar. Chem., 162, 71–76, 2014.

Lauvset, S. K., Gruber, N., Landschützer, P., Olsen, A., and Tjiputra, J.: Trends and drivers in global surface ocean pH over the past 3 decades, Biogeosciences, 12, 1285–1298, doi:10.5194/bg-12-1285-2015, 2015.

Le Quéré, C., Andrew, R. M., Friedlingstein, P., Sitch, S., Pongratz, J., Manning, A. C., Korsbakken, J. I., Peters, G. P., Canadell, J. G., Jackson, R. B., Boden, T. A., Tans, P. P., Andrews, O. D., Arora, V. K., Bakker, D. C. E., Barbero, L., Becker, M., Betts, R. A., Bopp, L., Chevallier, F., Chini, L. P., Ciais, P., Cosca, C. E., Cross, J., Currie, K., Gasser, T., Harris, I., Hauck, J., Haverd, V., Houghton, R. A., Hunt, C. W., Hurtt, G., Ilyina, T., Jain, A. K., Kato, E., Kautz, M., Keeling, R. F., Klein Goldewijk, K., Körtzinger, A., Landschützer, P., Lefèvre, N., Lenton, A., Lienert, S., Lima, I., Lombardozzi, D., Metzl, N., Millero, F., Monteiro, P. M. S., Munro, D. R., Nabel, J. E. M. S., Nakaoka, S.-I., Nojiri, Y., Padín, X. A., Peregon, A., Pfeil, B., Pierrot, D., Poulter, B., Rehder, G., Reimer, J., Rödenbeck, C., Schwinger, J., Séférian, R., Skjelvan, I., Stocker, B. D., Tian, H., Tilbrook, B., van der Laan-Luijkx, I. T., van der Werf, G. R., van Heuven, S., Viovy, N., Vuichard, N., Walker, A. P., Watson, A. J., Wiltshire, A. J., Zaehle, S., and Zhu, D.: Global Carbon Budget 2017, Earth Syst. Sci. Data, 10, 405-448, https://doi.org/10.5194/essd-10-405-2018, 2018.

Lewis, E., and Wallace, D. W. R.:Program Developed for CO2 System Calculations, *ORNL/CDIAC-105. Carbon Dioxide Information Analysis Center, Oak Ridge National Laboratory, US Department of Energy, Oak Ridge, Tennessee*, 1998.

Lueker, T. J., Dickson, A. G., and Keeling, C. D.: Ocean pCO2 calculated from dissolved inorganic carbon, alkalinity, and equations for K1 and K2: validation based on laboratory measurements of CO2 in gas and seawater at equilibrium, Mar.Chem., 70, 105–119, doi:10.1016/S0304-4203(00)00022-0, 2000.

McKinley, G. A., Fay, A. R. Takahashi, T., and Metzl, N.: Convergence of atmospheric and North Atlantic carbon dioxide trends on multidecadal timescales. Nature Geosc. doi:10.1038/NGEO1193, 2011.

McNeil, B., Matear, R., and Tilbrook, B.: Does carbon 13 track anthropogenic CO2 in Southern ocean, Glob. Biogeochem. Cycles,15, 597–613, 2001.

Mercier, H., Lherminier, P., Sarafanov, A., Gaillard, F., Daniault, N., Desbruyères, D.,Falina, A.,Ferron,B., Gourcuff, C., Huck, T., and Thierry, V.: Variability of the meridional overturning circulation at theGreenland–Portugal OVIDE section from 1993 to 2010, Prog. Oceanogr., 132, 250–261,doi:10.1016/j.pocean.2013.11.001, 2015.

Metzl, N., Corbière, A., Reverdin, G., Lenton, A., Takahashi, T., Olsen, A., Johannessen, T., Pierrot, D., Wanninkhof , R., Ólafsdóttir, S. R. Olafsson, J., and Ramonet, M.: Recent acceleration of the sea surface fCO2 growth rate in the North Atlantic subpolar gyre (1993 2008) revealed by winter observations, Glob. Biogeochem. Cycles, 24, GB4004, doi:10.1029/2009GB003658, 2010.

Millero, F. J., Lee, K., and Roche, M.: Distribution of alkalinity in the surface waters of the major oceans, Mar. Chem., 60(1-2), 111–130, doi: http://dx.doi.org/10.1016/S0304-4203(97)00084-4, 1998.

Nondal, G., Bellerby, R. G. J., Olsen, A., Johannessen, T., and Olafsson, J.: Optimal evaluation of the surface ocean CO2 system in the northern North Atlantic using data from voluntary observing ships, Limnol.and Oceanogr.: Methods, 7(1), 109–118, doi:10.4319/lom.2009.7.109, 2009.

Olafsson, J., Olafsdottir, S. R., Benoit-Cattin, A., and Takahashi, T.: The Irminger Sea and the Iceland Sea time series measurements of sea water carbon and nutrient chemistry 1983-2008. Earth Syst. Sci. Data 2, 99-104, 2010.

Olsen, A., Key, R. M., van Heuven, S., Lauvset, S. K., Velo, A., Lin, X., Schirnick, C., Kozyr, A., Tanhua, T., Hoppema, M., Jutterström, S., Steinfeldt, R., Jeansson, E., Ishii, M., Pérez, F. F.,and Suzuki, T.: The Global Ocean Data Analysis Project version 2 (GLODAPv2) - an internally consistent data product for the world ocean, Earth Syst.Sci.Data, 8, 297-323. doi:10.5194/essd-8-297-2016, 2016.

Olsen, A., Omar, A. M., Bellerby, R. G. J., Johannessen, T., Ninnemann,U., Brown, K. R., Olsson, K. A., Olafsson, J., Nondal, G.,Kivimäe, C., Kringstad, S., Neill, C., and Ólafsdóttir, S. R.: Magnitude and origin of the anthropogenic CO2 increase and Suesseffect in the Nordic seas since 1981, Glob. Biogeochem. Cycles,20, 1–12, doi:10.1029/2005GB002669, 2006.

Organelli, E., Barbieux, L., Claustre, H., Schmechtig, C., Poteau, A., Bricaud, A., Boss, E., Briggs, N., Dall'Olmo, G., D'Ortenzio, F., Lemayrie, E., Mangin, A., Oblensky, G., Penkerc'h, C., Prieur, L., Roesler, C., Serra, R.,Uitz, J., and Xing, W.: Two databases derived from BGC-Argo float measurements for marine biogeochemical and bio-optical applications. Earth Syst. Sci. data, 9, 861-880. Doi:10.5194/essd-9-861-2017, 2017.

Pierrot, D., Lewis, D. E.,and Wallace, D. W. R.: MS Excel Program Developed for CO2 System Calculations. ORNL/CDIAC-105a. Carbon Dioxide Information Analysis Center, Oak Ridge National Laboratory, U.S. Department of Energy, Oak Ridge, Tennessee. doi: 10.3334/CDIAC/otg.CO2SYS_XLS_CDIAC105a, 2006.

Pierrot, D., Neill, , Sullivan, K., Castle, R., Wanninkhof, R., Lüger, H., Johannessen, T., Olsen, A., Feely, R. A., and Cosca, C. E.: Recommendations for autonomous underway pCO2 measuring systems and data-reduction routines, Deep Sea Research Part II: Topical Studies in Oceanography,Volume 56, Issues 8–10,2009,Pages 512-522,ISSN 0967-0645, doi.org/10.1016/j.dsr2.2008.12.005, 2009.

Piron, A., Thierry, V., Mercier, H., and Caniaux, G.:Gyre-scale deep convection in the subpolar NorthAtlantic Ocean during winter 2014–2015, Geophys. Res. Lett., 44, 1439–1447,doi:10.1002/2016GL071895, 2017.

Quay, P., and Stutsman, J.: Surface layer carbon budget for the subtropical N. Pacific: d13C constraints at station ALOHA. Deep-Sea Res., I, 50, 1045-1061, 2003.

Racapé, V., Metzl, N., Pierre, C., Reverdin, G., Quay, P. D., and Olafsdottir, S. R.:The seasonal cycle of $\delta^{13}C_{DIC}$ in the North Atlantic subpolar gyre. Biogeosciences, 11, 1683-1692, doi:10.5194/bg-11-1683-2014, 2014.

Rahmstorf, S., Box, J. E., Feulner, G., Mann, M. E., Robinson, A., Rutherford, S., and Schaffernicht, E. J.: Exceptional twentieth-century slowdown in Atlantic Ocean overturning circulation. Nature Clim.Change, 5(5), 475–480. http://doi.org/10.1038/nclimate2554, 2015.

Reverdin, G.: North Atlantic subpolar gyre surface variability (1895-2009). J. Climate, 17, 4571-4584. Doi:10.1175/2010JCLI3493.1, 2010.

Reverdin, G.,Metzl, N.,Corbière, A.: Carbon dioxide measurement results in the north Atlantic subploar gyre during SURATLANT cruise AGSK20040110. *Laboratoire d'Océanographie et du Climat: Expérimentation et Approches Numériques, Université Pierre-et-Marie-Curie, France*, Unpublished dataset #603247 : https://doi.pangaea.de/10.1594/PANGAEA.603247, 2007.

Reverdin, G.,Ólafsdóttir, S. R.,Metzl, N.: Hydrochemistry measured on water bottle samples in the North Atlantic subpolar gyre during SURATLANT cruise 64RJ20130704. *PANGAEA*, https://doi.org/10.1594/PANGAEA.844132, 2015.

Reverdin, G., Valdimarsson, H., Alory, G., Diverres, D., Bringas, F., Goni, G., Heilmann, L., Chafik, L., and Szekely, T.: North Atlantic subpolar gyre along predetermined ship tracks since 1993: a monthly dataset of surface temperature, salinity, and density. Submitted to ESSD, 2018.

Robson, Ortega, J. P., and Sutton, R.: A reversal of climate trends in the North Atlantic since 2005. Nature Geosci., 9, 513-517, doi:10.1038/ngeo2727, 2016.

Rödenbeck, C., Bakker, D. C. E., Gruber, N., Iida, Y., Jacobson, A.R., Jones, S., Landschützer, P., Metzl, N., Nakaoka, S., Olsen, A., Park, G.-H., Peylin, P., Rodgers, K. B., Sasse, T. P., Schuster, U., Shutler, J. D., Valsala, V., Wanninkhof, R., Zeng, J.. Data-based estimates of the ocean carbon sink variability – First results of the Surface Ocean pCO2 Mapping intercomparison (SOCOM). Biogeosciences 12: 7251-7278. doi:10.5194/bg-12-7251-2015., 2015

Rödenbeck, C., Bakker, D. C. E., Metzl, N., Olsen, A., Sabine, C., Cassar, N., Reum, F., Keeling, R. F., and Heimann, M.: Interannual sea–air CO_2 flux variability from an observation-driven ocean mixed-layer scheme.Biogeosciences, 11, 4599-4613, 2014 doi:10.5194/bg-11-4599-2014, 2014.

Rossby, T., Reverdin, G., Chafik, L., and Soiland, H.:A direct estimate of poleward volume, heat and fresh water fluxes at 59.5°N between Greenland and Scotland. J. Geophys. Res.: Oceans. http://dx.doi.org/10.1002/2017JC012835, 2017.

Schuster, U., McKinley, G. A., Bates, N., Chevallier, F., Doney, S. C., Fay, A. R., González Dávila, M., Gruber, N., Jones, S., Krijnen, J., Landschützer, P., Lefèvre, N., Manizza, M., Mathis, J. Metzl, N., Olsen, A., Rios, A. F., Rödenbeck, C., Santana-Casiano, J. M., Takahashi, T., Wanninkhof, R., and Watson, A. J.: An assessment of the Atlantic and Arctic sea-air CO2 Fluxes, 1990-2009. Biogeosciences, 10, 607-627, doi:10.5194/bg-10-607-2013, 2013.

Signorini, S. R., Häkkinen, S., Gudmundsson, K., Olsen, A., Omar, A. M., Olafsson, J., Reverdin, G., Henson, S. A., McClain, C. R., and Worthen, D. L.: The role of phytoplankton dynamics in the seasonal and interannual variability of carbon in the subpolar North Atlantic – A modeling study. Geosci. Model Dev.,5,683-707,doi:10.5194/gmd-5-683-2012, 2012.

Skrzypek, G., and Ford, D.: Stable Isotope analysis of saline water samples on a cavity 546 ring-down spectroscopy instrument. Environm. Sci.andTech., 48(5), 2827–2834, 2014.

Sonnerup, R. E. and Quay, P. D.: 13C constraints on oceancarbon cycle models, Glob. Biogeochem.

Cycles, 26, GB2014,doi:10.1029/2010GB003980, 2012.

Tagliabue, A. and Bopp, L.: Towards understanding global variability in ocean carbon-13, Glob. Biogeochem. Cycles, 22, GB1025,doi:10.1029/2007GB003037, 2008.

Takahashi, T., Sutherland, S. C., Sweeney, C., Poisson, A., Metzl, N., Tilbrook, B., Bates, N., Wanninkhof, R., Feely, R. A., Sabine, C., Olafsson, J., and Nojiri, Y.:Global Sea-Air CO2 Flux Based on Climatological Surface Ocean pCO2, and Seasonal Biological and Temperature Effect.Deep-Sea Res. II, 49, 9-10, 1601-1622, 2002.

Takahashi, T., Sutherland, S. C., Wanninkhof, R., Sweeney, C., Feely, R. A., Chipman, D. W., Hales, B., Friederich, G., Chavez, F., Sabine, C., Watson, A. J., Bakker, D. C., Schuster, U., Metzl, N., Yoshikawa-Inoue, H., Ishii, M., Midorikawa, T., Nojiri, Y., Körtzinger, A., Steinhoff, T., Hoppema, M., Olafsson, J., Arnarson, T. S., Tilbrook, B., Johannessen, T., Olsen, A., Bellerby, R., Wong, C., Delille, B., Bates, N., and de Baar, H. J.: Climatological mean and decadal change in surface ocean pCO2, and net sea air CO2 flux over the global oceans , Deep-Sea Res. II,56(8-10), 554–577, doi:http://dx.doi.org/10.1016/j.dsr2.2008.12.009, 2009.

Takahashi, T., Sutherland, S. C., Chipman, D. W., Goddard, J. G., Cheng Ho, Newberger, T., Sweeney, C.,and Munro, D. R.: Climatological Distributions of pH, pCO_2, Total CO_2, Alkalinity, and $CaCO_3$ Saturation in the Global Surface Ocean, and Temporal Changes at Selected Locations. Marine Chemistry. doi: 10.1016/j.jmarchem.2014.06.004, 2014.

Vangriesheim A., Pierre, C., Aminot A., Metzl, N., Baurand, F., and Caprais, J.-C.: The influence of Congo River discharges in the surface and deep layers of the Gulf of Guinea. Deep-Sea Res. II,56, 2183-2196, doi: 10.1016/j.dsr2.2009.04.002, 2009.

Wanninkhof, R., and J. Trinanes, J.:The impact of changing wind speeds on gas transfer and its effect on global air-sea CO_2 fluxes, Global Biogeochem. Cycles, 31, *doi:*10.1002/2016GB005592, 2017.

Watson, A.J., U. Schuster, D .C. E. Bakker, N. Bates, A. Corbiere, M. Gonzalez-Davila, T. Freidrich, J. Hauck, C. Heinze, T. Johannessen,A. Koertzinger, N. Metzl, J. Olafsson, A. Olsen, A. Oschlies, X. Padin, B. Pfeil, A. Rios, M Santana-Casiano, T. Steinhoff, M. Telszewski, D. W. R. Wallace, R. Wanninkhof. Tracking the variable North Atlantic sink for atmospheric CO_2, *Science*, 326, 1391, doi:10.1126/science.1177394, 2009

Weiss, R., and Price, B.: Nitrous oxide solubility in water and seawater, Marine Chemistry, 8, 347–359, 1980.

Yashayaev, I., and Loder, J. W.:Recurrent replenishment of Labrador Sea water and associated decadal-scale variability. J. Geophys. Res., 8095-8114, doi:10.1002/2016JC012046, 2016.

Zunino, P., Garcia-Ibañez, M. I., Lherminier, P., Mercier, H., Rios, A. F., and Pérez, F. F. : Variability of the transport of anthropogenic CO_2 at the Greenland–Portugal OVIDE section: controlling mechanisms, Biogeosciences, 11, 2375-2389, https://doi.org/10.5194/bg-11-2375-2014, 2014.

Earth Syst. Sci. Data Discuss., https://doi.org/10.5194/essd-2018-50
Manuscript under review for journal Earth Syst. Sci. Data
Discussion started: 24 April 2018

Open Access Earth System Science Data Discussions

Figure and table captions

Table A1: Comparisons of DIC and A_t samples shared between LOCEAN and other institutes (1, 2, 3, 4). Institute 1 uses a manometric method for measuring DIC, institutes 2, 3 and 4 use a potentiometric method for DIC, whereas institutes 3 and 4 use a potentiometric method for A_t. The different columns are for institute number, months and year of sampling, number of samples, average and rms diff (LOCEAN-other) first for DIC, then for A_t.

Figure 1: monitoring of the surface subpolar gyre. SURATLANT is along ship track AX2. The red currents indicate a schematic view of surface circulation in the subpolar gyre originating from the Gulf Stream and North Atlantic Current. The blue lines indicate the path of the freshest waters of polar or continental origin, and the purple arrows illustrate the deep export circulation.

Figure 2: Left panel spatial distribution of the A_t samples collected in 2001-2016 and used to estimate a regression to salinity (for S > 34 psu) (color corresponds to A_t value). Right panel: A_t-S dispersion diagram. The red line corresponds to A_t=46.2543*S+687.741 best fit (with rms = 8.4 µmol kg^{-1}, R^2=0.84 and n=1332 for S> 34)

Figure 3: Average seasonal cycle in 2001-2017. For DIC, A_t, $\delta^{18}O$, PO_4, NO_3, Si, it is normalized for S variations and reported at S=35. The colour of the curves correspond to the geographical boxes presented in upper right corner (yellow, red, green, blue, black from south to north; the black trajectory correspond to January 2017 sampling). Yellow curves (south) for S and $\delta^{18}O$ and DIC have been shifted. A map with the location of the boxes is also provided.

Figure 4: Seasonal cycles of fCO2 (a) and pH (b) in each box. On (a) the purple dashed-line is the mean monthly atmospheric fCO2 derived from CO2 concentrations at Mace-Head station for year 2010.

Figure 5: Seasonal cycles of fCO_2 (a) , A_t (b), DIC (c) and pH (d) derived from SURATLANT data and the climatology (Takahashi et al., 2014) for the central region (boxes 54-58°N and 58-62°N).

Figure 6: Time-series of A_t observed in the latitudinal band 50-63°N. For 1993-1997 A_t was derived from Salinity. The brown line depicts the long-term trend (+0.02 µmol $kg^{-1}yr^{-1}$), i.e. no trend detected for A_t. Low A_t values (< 2250 µmol kg^{-1}) observed near 50°N. The color corresponds to calendar month (right scale).

Figure 7: Time-series of DIC observed in the latitudinal band 50-63°N for winter (January-March, left) and summer (June-September, right). The dashed lines depict the long-term trend (+0.72 µmol kg^{-1} yr^{-1} in winter, +0.67 µmol kg^{-1} yr^{-1}in summer,). The color corresponds to calendar month (right scale).

Figure 8: Time-series of fCO_2 observed in the latitudinal band 50-63°N for winter (January-March, left) and summer (June-September, right). The dashed lines depict the long-term trend (+1.67 µatm yr^{-1}in winter and +2.1 µatm yr^{-1}in summer).The color corresponds to calendar month (right scale).

Figure 9: Time-series of fCO_2 (left) and delta-fCO_2 (right) for all SURATLANT data. The brown lines depict the long-term trends (+1.9 µatm yr^{-1} on left panel, -0.04 µatm yr^{-1} on right panel).The color corresponds to calendar month (right scale).

Figure 10: Time-series of pH SURATLANT data. The brown line depicts the long-term trend (-0.002

yr^{-1}). Note high pH (> 8.2) observed in coastal regions (north or south).The color corresponds to calendar month (right scale).

Figure 11: trend for $\delta^{13}C_{DIC}$. left panel, data distribution (2005-2017); right, time series with trend for summer season (red dashed line: trend -0.042 yr^{-1}), trend for winter season(blue dashed line, trend, -0.015yr^{-1}), all seasons (brown dashed line, trend -0.022 yr^{-1}) (notice that data have been adjusted by+0.05 in 2005-2006 and by +0.13 since 2010). The color on left panel corresponds to $\delta^{13}C_{DIC}$value and on right panel corresponds to the calendar month (right scale).

Figure A1: (a) fCO2 calculated versus fCO2 measured (µatm) for 172 colocated samples. Dashed line: fCO2-SUR= 1.05 fCO2-AOML (r2=0.9) (b) fCO2 differences versus fCO2 measured for same samples (µatm)

Figure B1: Comparison of using calculated A_t (with SURATLANT relationship) with using measured A_t. Left panel, difference in A_t (calculated – measured), middle panel difference in fCO_2 and right panel, difference in pH.

Figure B2: scatter diagram of SURATLANT A_t versus S. Different linear fits are also presented. The blue line corresponds to the relationship adopted in this study and the red line to the Nondal et al. (2009) relationship.

Figure B3: Difference in fCO2 estimated when using A_t derived from S with SURATLANT relationship and when using A_t derived from S with Nondal et al. (2009) relationship. Plot of diff(fCO2) as a function of salinity for all SURATLANT samples.

Figure C1: Hövmüller diagram along AX2 (left, Newfoundland; right, Iceland) of S' (left, psu) and T' (right, °C) deviations from an average seasonal cycle in July 1993-June 2017.

Figure C2: January-April salinity deviations from the seasonal cycle near 60°N. In red, from the monthly analysis (see Fig. C1), and in blue from the discrete salinity samples (for those, the analysed seasonal cycle is presented on Fig. 3).

Earth Syst. Sci. Data Discuss., https://doi.org/10.5194/essd-2018-50
Manuscript under review for journal Earth Syst. Sci. Data
Discussion started: 24 April 2018

Open Access Earth System Science Data Discussions

Table A1: Comparisons of DIC and A_t samples shared between LOCEAN and other institutes (1, 2, 3, 4). Institute 1 uses a manometric method for measuring DIC, institutes 2, 3 and 4 use a potentiometric method for DIC, whereas institutes 3 and 4 use a potentiometric method for A_t. The different columns are for institute number, months and year of sampling, number of samples, average and rms diff (LOCEAN-other) first for DIC, then for A_t.

institute	Month/year	N samples	Average diff	Sigma	N samples	Average Diff	sigma
1	01/2005-11/2006	115	-4.1	6.8			
2	6-8/2010	15	-7.4	3.5			
3	8/2010	9	-5.4	3.1	10	-1.5	4.1
4	8/2010	9	-5.9	4.0	10	1.4	4.8
3	1/2015	8	-6.8	3.6	8	0.0	7.3
2	4-10/2016	8	-1.2	5.3			

Earth Syst. Sci. Data Discuss., https://doi.org/10.5194/essd-2018-50
Manuscript under review for journal Earth Syst. Sci. Data
Discussion started: 24 April 2018

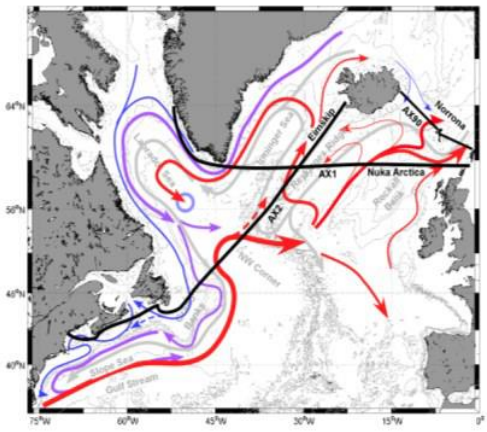

Figure 1: Monitoring of the surface subpolar gyre. SURATLANT is along ship track AX02. The red currents indicate a schematic view of surface circulation in the subpolar gyre originating from the Gulf Stream and North Atlantic Current. The blue lines indicate the path of the freshest waters of polar or continental origin, and the purple and grey arrows illustrate the deep export circulation.

Earth Syst. Sci. Data Discuss., https://doi.org/10.5194/essd-2018-50
Manuscript under review for journal Earth Syst. Sci. Data
Discussion started: 24 April 2018

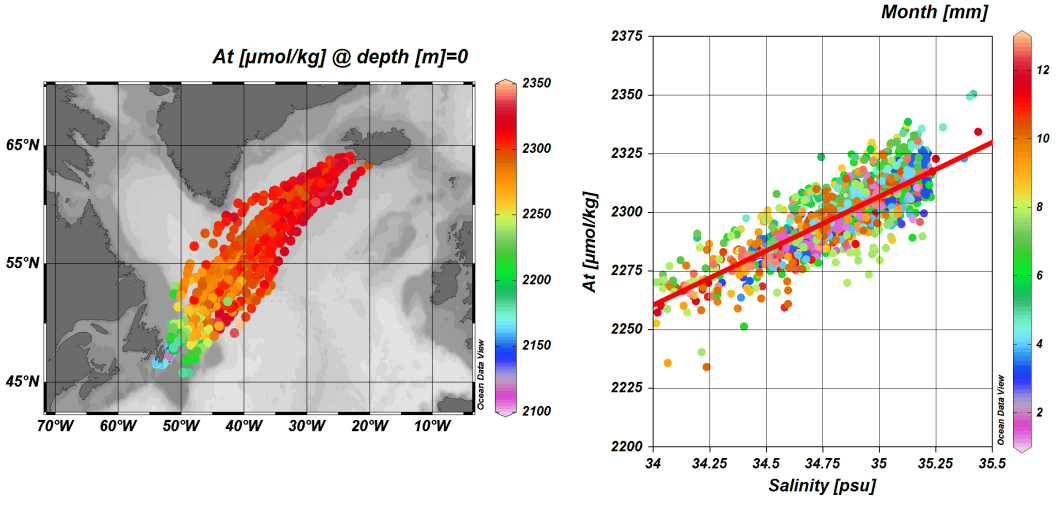

Figure 2: Left panel spatial distribution of the A_t samples collected in 2001-2016 and used to estimate a regression to salinity (for S > 34 psu) (color corresponds to A_t value). Right panel: A_t-S dispersion diagram. The red line corresponds toA_t=46.2543*S+687.741best fit (with rms = 8.4 µmol kg^{-1}, R^2=0.84 and n=1332 for S> 34)

Earth Syst. Sci. Data Discuss., https://doi.org/10.5194/essd-2018-50
Manuscript under review for journal Earth Syst. Sci. Data
Discussion started: 24 April 2018

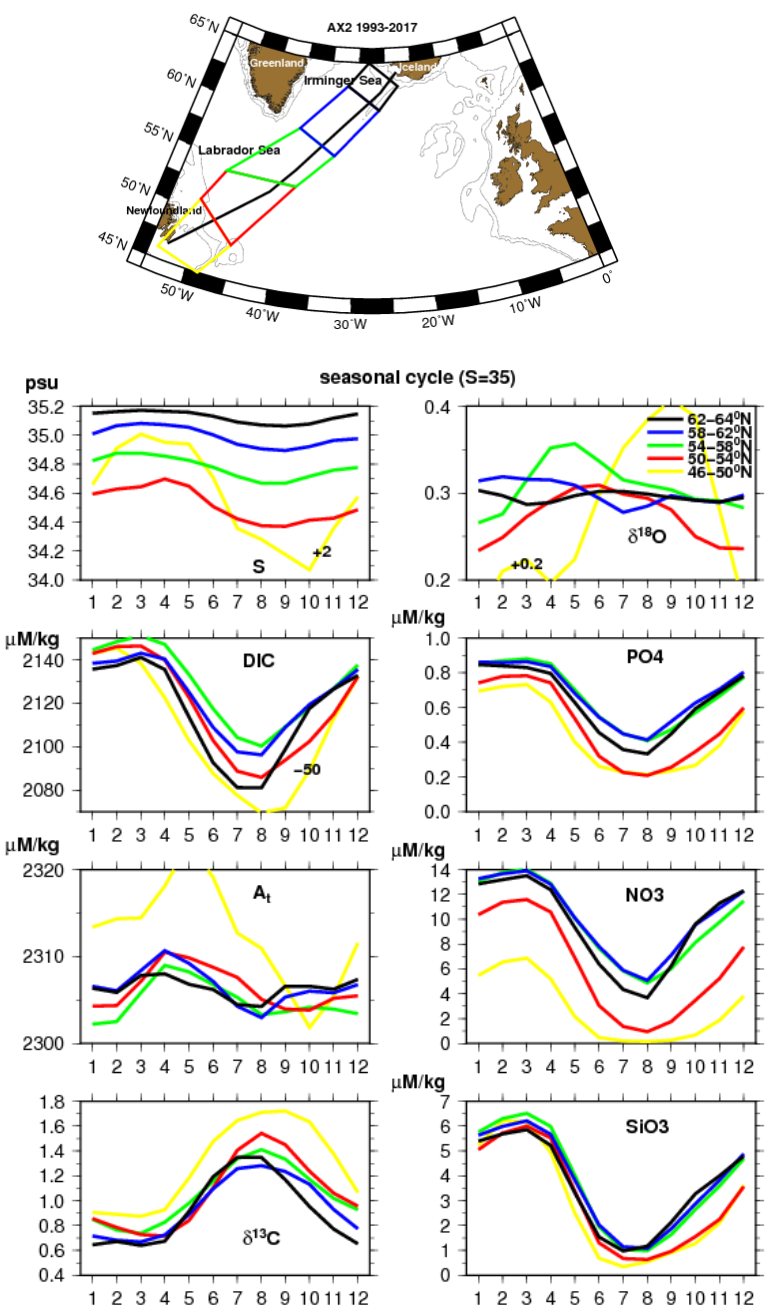

Figure 3: Average seasonal cycle in 2001-2017. For DIC, A_t, $\delta^{18}O$, PO_4, NO_3, Si, it is normalized for S variations and reported at S=35. The colour of the curves correspond to geographical boxes presented in upper right corner (yellow, red, green, blue, black from south to north; the black trajectory correspond to January 2017 sampling). Yellow curves (south) for S and $\delta^{18}O$ and DIC have been shifted. A map with the location of the boxes is also provided.

Earth Syst. Sci. Data Discuss., https://doi.org/10.5194/essd-2018-50
Manuscript under review for journal Earth Syst. Sci. Data
Discussion started: 24 April 2018

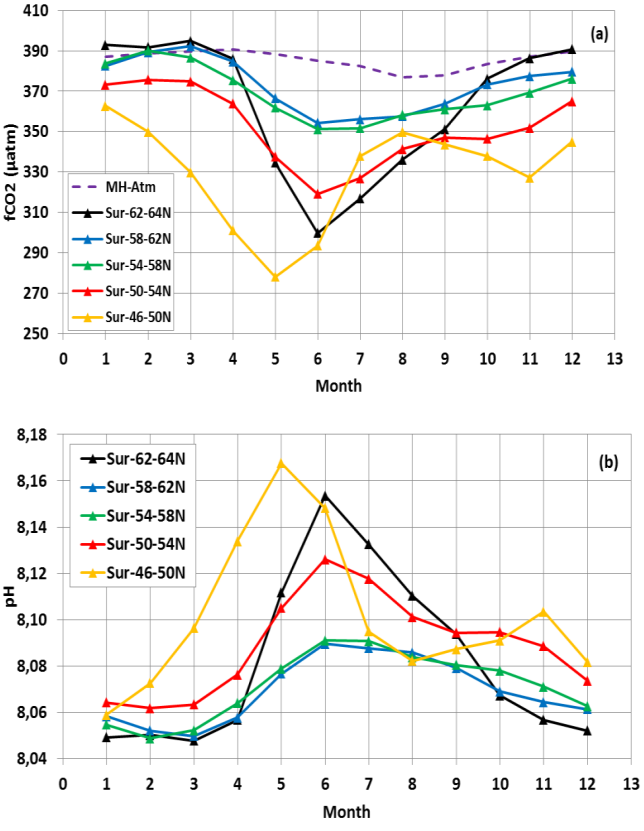

Figure 4: Seasonal cycles of fCO_2 (a) and pH (b) in each box. On (a) the purple dashed-line is the mean monthly atmospheric fCO_2 derived from CO_2 concentrations at Mace-Head station for year 2010.

Earth Syst. Sci. Data Discuss., https://doi.org/10.5194/essd-2018-50
Manuscript under review for journal Earth Syst. Sci. Data
Discussion started: 24 April 2018

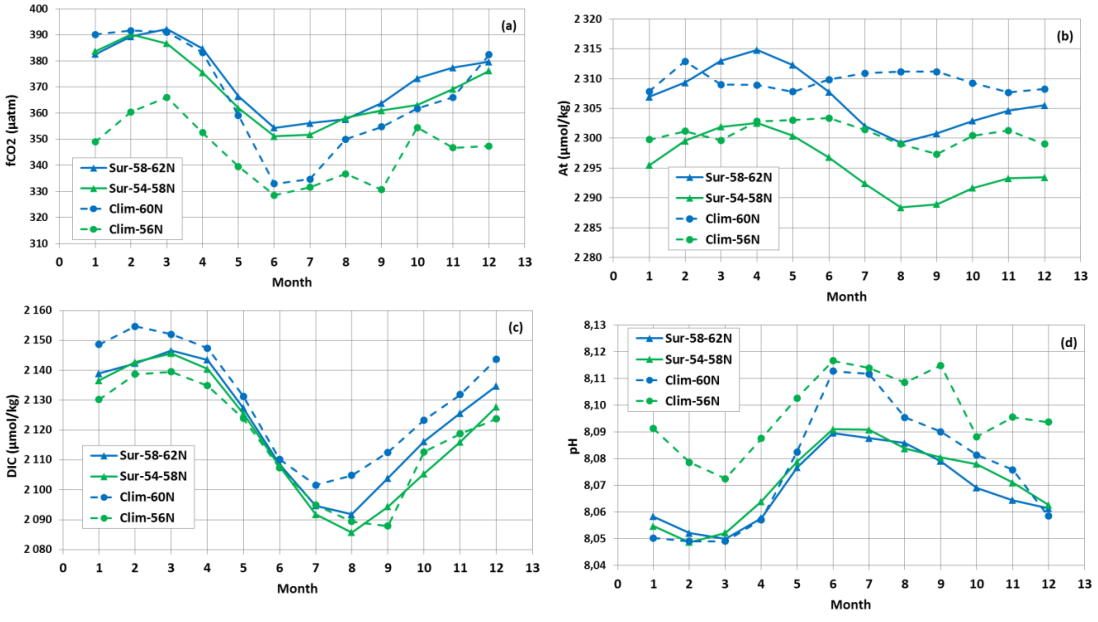

Figure 5: Seasonal cycles of fCO_2 (a), A_t (b), DIC (c) and pH (d) derived from SURATLANT data and the climatology (Takahashi et al., 2014) for the central region (boxes 54-58°N and 58-62°N).

Earth Syst. Sci. Data Discuss., https://doi.org/10.5194/essd-2018-50
Manuscript under review for journal Earth Syst. Sci. Data
Discussion started: 24 April 2018

Open Access Earth System Science Data Discussions

1307
1308

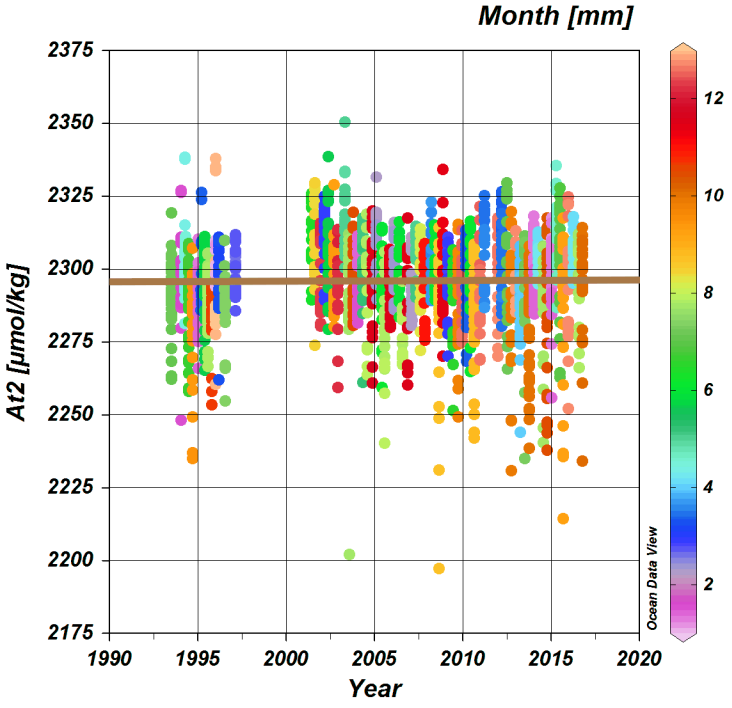

Figure 6: Time-series of A_t observed in the latitudinal band 50-63°N. For 1993-1997 A_t was derived from Salinity. The brown line depicts the long-term trend (+0.02µmol kg^{-1} yr^{-1}), i.e. no trend detected for A_t. Low A_t values (< 2250 µmol kg^{-1}) observed near 50°N.The color corresponds to calendar month (right scale).

Earth Syst. Sci. Data Discuss., https://doi.org/10.5194/essd-2018-50
Manuscript under review for journal Earth Syst. Sci. Data
Discussion started: 24 April 2018

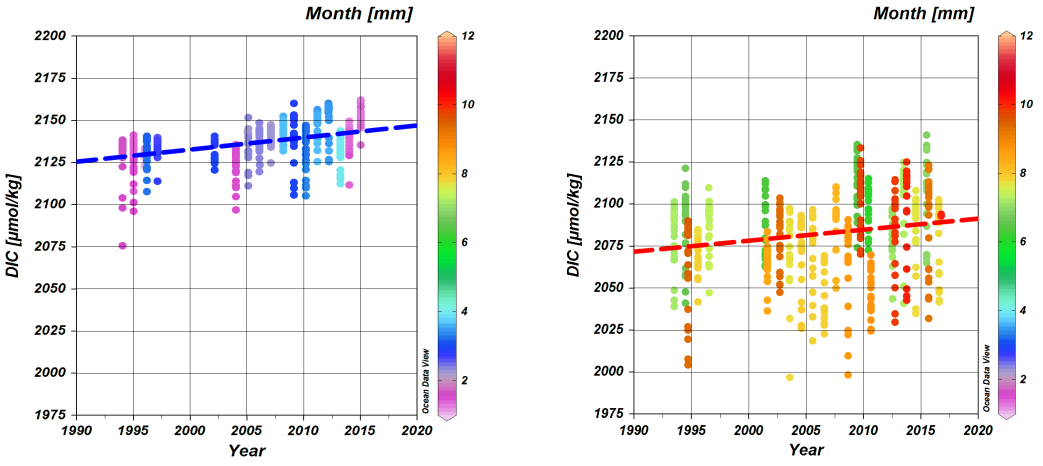

Figure 7: Time-series of DIC observed in the latitudinal band 50-63°N for winter (January-March, left) and summer (June-September, right). The dashed lines depict the long-term trend (+0.72µmol kg^{-1} yr^{-1} in winter, +0.67µmol kg^{-1} yr^{-1} in summer). The color corresponds to calendar month (right scale).

Earth Syst. Sci. Data Discuss., https://doi.org/10.5194/essd-2018-50
Manuscript under review for journal Earth Syst. Sci. Data
Discussion started: 24 April 2018

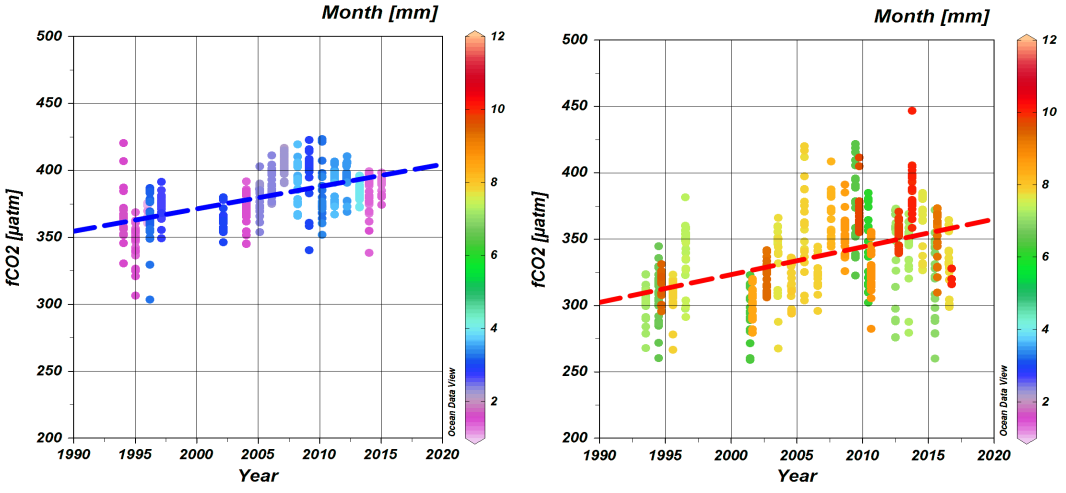

Figure 8: Time-series of fCO_2 observed in the latitudinal band 50-63°N for winter (January-March, left) and summer (June-September, right). The dashed lines depict the long-term trend (+1.67 µatm yr^{-1} in winter and +2.1 µatm yr^{-1} in summer).The color corresponds to calendar month (right scale).

Earth Syst. Sci. Data Discuss., https://doi.org/10.5194/essd-2018-50
Manuscript under review for journal Earth Syst. Sci. Data
Discussion started: 24 April 2018

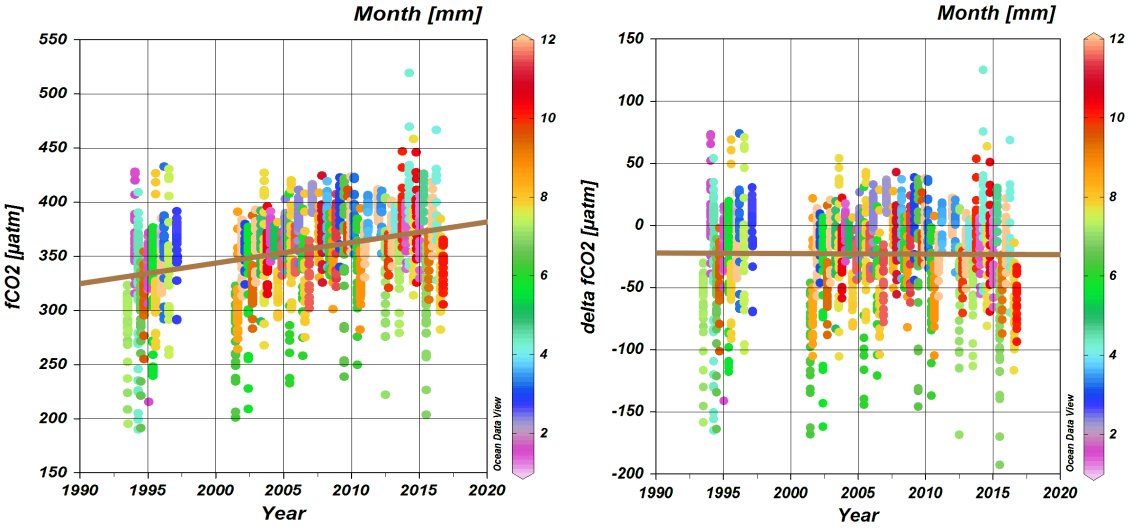

Figure 9: Time-series of fCO_2 (left) and delta-fCO_2 (right) for all SURATLANT data. The brown lines depict the long-term trends (+1.9 µatm yr^{-1} on left panel, -0.04 µatm yr^{-1} on right panel).The color corresponds to calendar month (right scale).

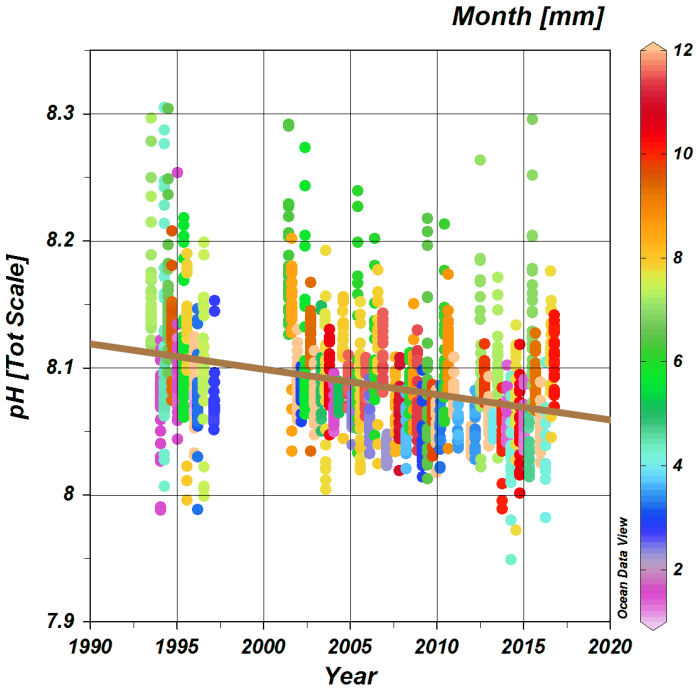

Figure 10 : Time-series of pH SURATLANT data. The brown line depicts the long-term trend (-0.002 yr^{-1}). Note high pH (> 8.2) observed in coastal regions (north or south).The color corresponds to calendar month (right scale).

Earth Syst. Sci. Data Discuss., https://doi.org/10.5194/essd-2018-50
Manuscript under review for journal Earth Syst. Sci. Data
Discussion started: 24 April 2018

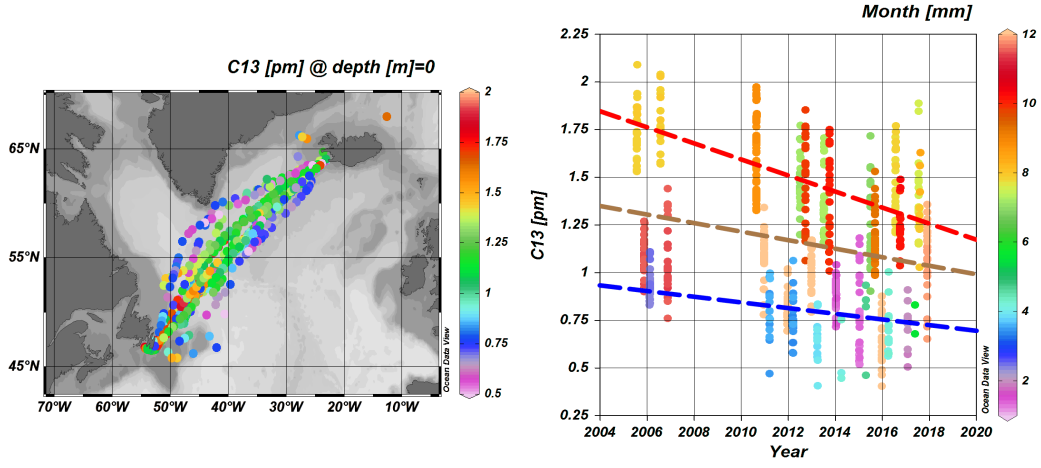

Figure 11: trend for $\delta^{13}C_{DIC}$. left panel, data distribution (2005-2017); right, time series with trend for summer season (red dashed line: trend -0.042 yr^{-1}), trend for winter season(blue dashed line, trend, -0.015 yr^{-1}), all seasons (brown dashed line, trend -0.022 yr^{-1})(notice that data have been adjusted by+0.05 in 2005-2006 and by +0.13 since 2010). The color on left panel corresponds to $\delta^{13}C_{DIC}$value and on right panel corresponds to the calendar month (right scale).

Earth Syst. Sci. Data Discuss., https://doi.org/10.5194/essd-2018-50
Manuscript under review for journal Earth Syst. Sci. Data
Discussion started: 24 April 2018

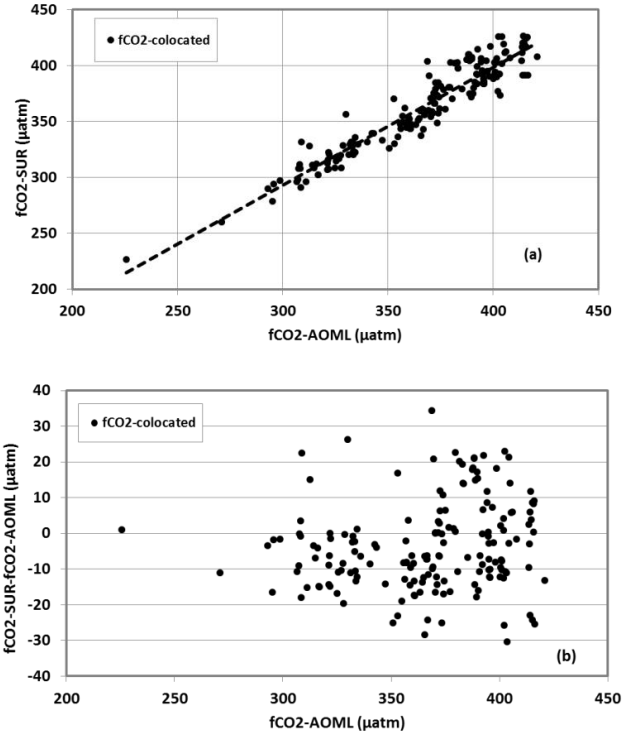

Figure A1: (a) fCO_2 calculated versus fCO_2 measured (µatm) for 172 colocated samples. Dashed line: fCO_2-SUR= 1.05 fCO_2-AOML (r2=0.9) (b) fCO_2 differences versus fCO_2 measured for same samples (µatm)

Earth Syst. Sci. Data Discuss., https://doi.org/10.5194/essd-2018-50
Manuscript under review for journal Earth Syst. Sci. Data
Discussion started: 24 April 2018

Open Access Earth System Science Data Discussions

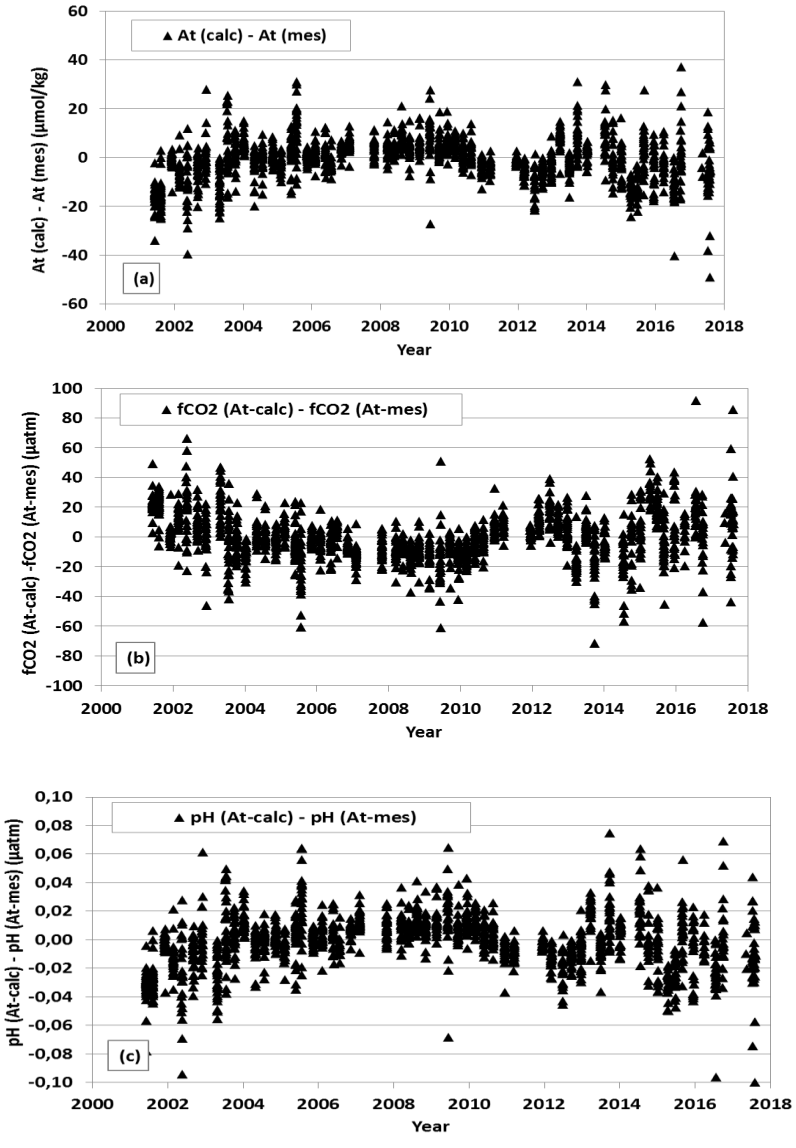

Figure B1: Comparison of using calculated A_t (with SURATLANT relationship) with using measured A_t. Left panel, difference in A_t (calculated – measured), middle panel difference in fCO_2 and right panel, difference in pH.

Earth Syst. Sci. Data Discuss., https://doi.org/10.5194/essd-2018-50
Manuscript under review for journal Earth Syst. Sci. Data
Discussion started: 24 April 2018

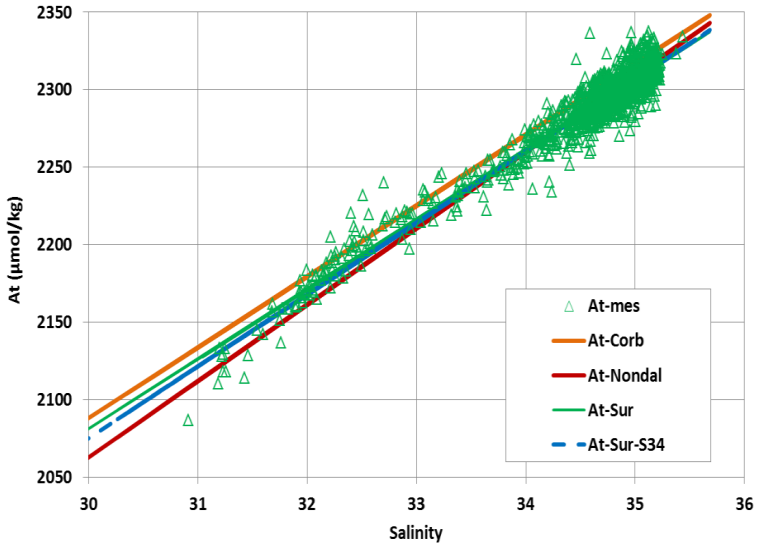

Figure B2: scatter diagram of SURATLANT A_t versus S. Different linear fits are also presented. The blue line corresponds to the relationship adopted in this study and the red line to the Nondal et al. (2009) relationship.

Earth Syst. Sci. Data Discuss., https://doi.org/10.5194/essd-2018-50
Manuscript under review for journal Earth Syst. Sci. Data
Discussion started: 24 April 2018

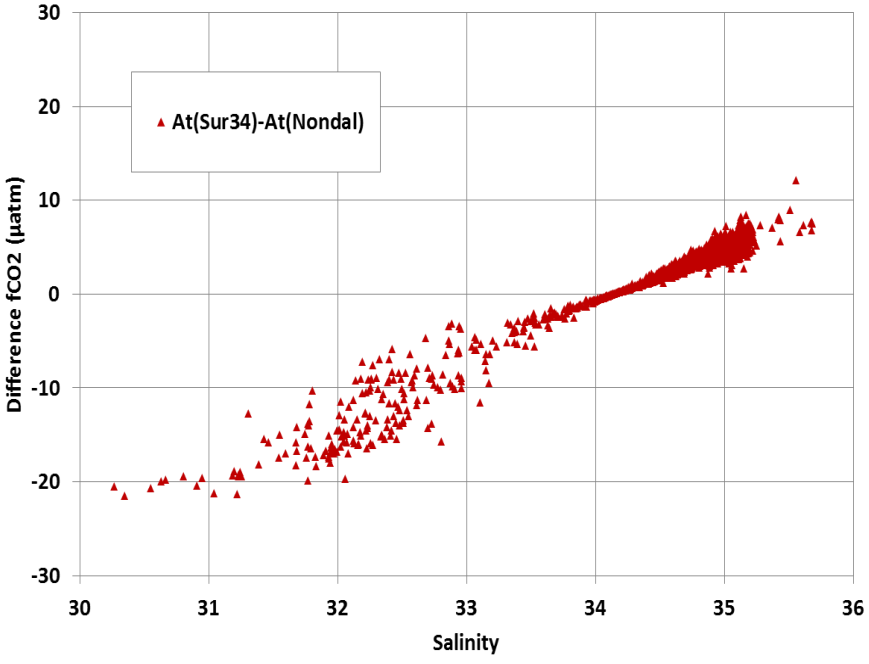

Figure B3: Difference in fCO_2 estimated when using A_t derived from S with SURATLANT relationship and when using A_t derived from S with Nondal et al. (2009) relationship. Plot of diff(fCO2) as a function of salinity for all SURATLANT samples.

Earth Syst. Sci. Data Discuss., https://doi.org/10.5194/essd-2018-50
Manuscript under review for journal Earth Syst. Sci. Data
Discussion started: 24 April 2018

Open Access Earth System Science Data Discussions

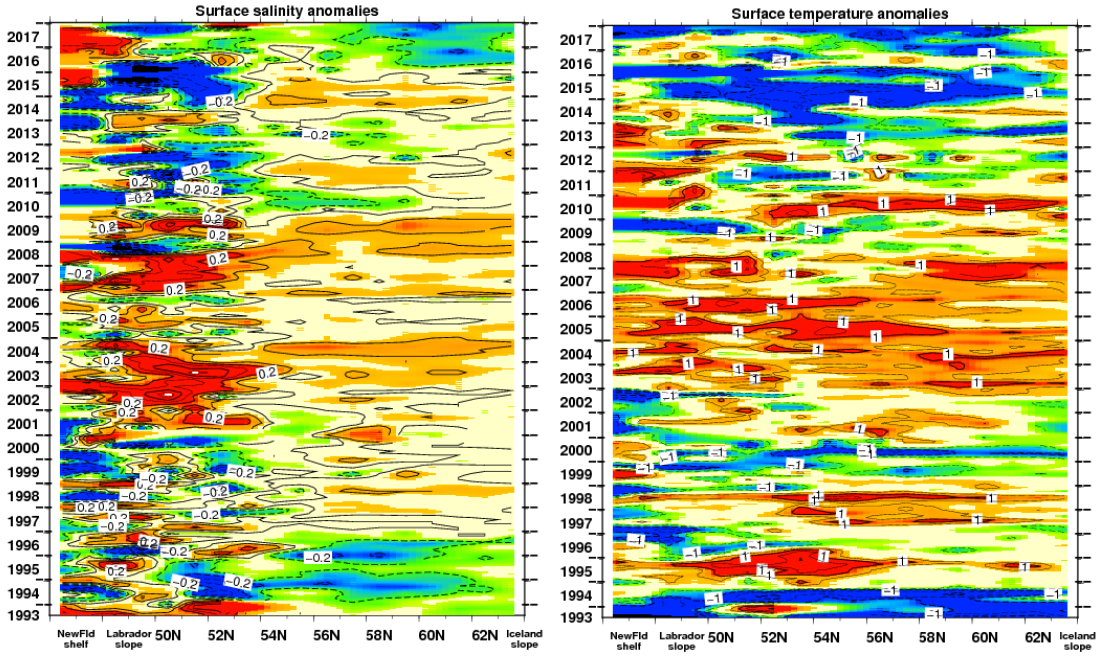

Figure C1: Hövmüller diagram along AX2 (left, Newfoundland; right, Iceland) of S' (left, psu) and T' (right, °C) deviations from an average seasonal cycle in July 1993-December 2017.

Earth Syst. Sci. Data Discuss., https://doi.org/10.5194/essd-2018-50
Manuscript under review for journal Earth Syst. Sci. Data
Discussion started: 24 April 2018

Open Access Earth System Science Data Discussions

1622

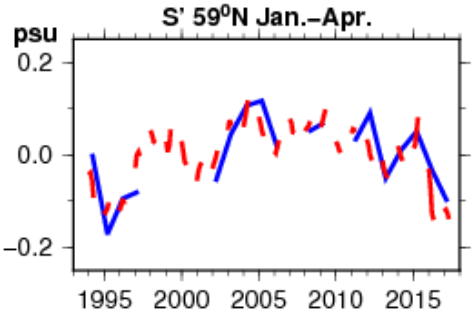

1623
1624 **Figure C2**: January-April salinity deviations from the seasonal cycle near 59°N. In red, from the
1625 monthly analysis (see Fig. C1), and in blue from the discrete salinity samples (for those, the analysed
1626 seasonal cycle is presented on Fig. 3).
1627